

Reviews of Geophysics

REVIEW ARTICLE

10.1029/2018RG000631

Key Points:

- Antarctic sea ice has a remarkably consistent, asymmetric annual cycle, despite substantial interannual variability
- Zonal winds work with or against the evolving position of the ice edge, and ice-ocean albedo feedback amplifies the sea ice seasonal cycle
- Climate models tend to capture the pattern and timing of the Antarctic seasonal cycle but not the magnitude

Correspondence to:

C. Eayrs,
clare.eayrs@nyu.edu

Citation:

Eayrs, C., Holland, D. M., Francis, D., Wagner, T. J. W., Kumar, R., & Li, X. (2019). Understanding the seasonal cycle of Antarctic sea ice extent in the context of longer-term variability. *Reviews of Geophysics*, 57. <https://doi.org/10.1029/2018RG000631>

Received 10 NOV 2018

Accepted 19 JUL 2019

Accepted article online 30 JUL 2019

Understanding the Seasonal Cycle of Antarctic Sea Ice Extent in the Context of Longer-Term Variability

Clare Eayrs¹ , David Holland^{1,2} , Diana Francis¹ , Till Wagner³ , Rajesh Kumar¹, and Xichen Li⁴

¹Center for Global Sea Level Change, New York University Abu Dhabi, Abu Dhabi, United Arab Emirates, ²Courant Institute of Mathematical Sciences, New York University, New York, NY, USA, ³Department of Physics and Physical Oceanography, University of North Carolina at Wilmington, Wilmington, NC, USA, ⁴Institute of Atmospheric Physics, Beijing, China

Abstract Over the 40-year satellite record, there has been a slight increasing trend in total annual mean Antarctic sea ice extent of approximately 1.5% per decade that is made up of the sum of significantly larger opposing regional trends. However, record increases in total Antarctic sea ice extent were observed during 2012–2014, followed by record lows (for the satellite era) through 2018. There is still no consensus on the main drivers of these trends, but it is generally believed that the atmosphere plays a significant role and that seasonal time scales and regional scale processes are important. Despite considerable yearly and regional variability, the mean seasonal cycle of growth and melt of Antarctic sea ice is strikingly consistent, with a slow growth but fast melt season. If we are to project trends in Antarctic sea ice and understand changes on longer time scales, we need to understand the mechanisms related to the seasonal cycle separately from those that drive variability. Twice-yearly changes in the position and intensity of the zonal winds circling Antarctica are thought to drive the system by working with or against the evolving sea ice edge to slow the autumn advance and hasten the spring melt. Open water regions, created by divergence associated with the zonal winds, amplify the spring melt through increased warming of the upper ocean. Climate models fail to accurately reproduce mean Antarctic sea ice extent and overestimate its year-to-year variability, but they tend to capture the pattern and timing of the Antarctic seasonal cycle.

Plain Language Summary Antarctic sea ice extent has been observed daily from satellites over the last 40 years. Compared to the Arctic, there has been little overall change in Antarctic sea ice cover over this time. However, the slightly increasing trend masks substantial interannual and regional variability, and recent years have seen record increases (2012–2014) followed by record lows (through 2018). Despite this variability, the pattern of growth and melt of total Antarctic sea ice shows a consistent, asymmetric cycle with slow growth but rapid melt periods. The presence of many individual storms around the continent gives rise to a band of low pressure that circles the continent, and this low-pressure band marks a boundary between westerlies to the north and easterlies to the south. Twice-yearly changes in the position and intensity of these zonal winds work with or against the evolving ice edge to slow the autumn advance and hasten the spring retreat. Open water areas created in the spring lead to increased warming of the upper ocean, which also acts to speed up the spring retreat. On the whole, climate models tend to capture the pattern and timing, but not the magnitude, of the Antarctic seasonal cycle.

1. Introduction

Sea ice is a critical component of the climate system: The seasonal cycle of sea ice affects global climate dynamics through its interplay with the planetary albedo, atmospheric circulation, ocean productivity, and thermohaline circulation. It has been known since the start of the satellite record (November 1978) that Antarctic sea ice exhibits high regional and seasonal variability (Zwally et al., 1983), and large interannual variability in total annual mean Antarctic sea ice extent (SIE) is seen throughout this record (Gloersen et al., 1992; Parkinson & Cavalieri, 2012). Overall, this record exhibits a slight increasing trend in total Antarctic SIE of approximately 1.5% per decade, with record highs observed during 2012–2014, then followed by decreases in 2016, 2017, and 2018 (Macalady & Thomas, 2017; Meehl et al., 2019). These gross changes are the result of opposing trends in different sectors of the Southern Ocean (Holland, 2014; Holland & Kwok, 2012), with pockets of strongly positive and negative trends occurring in near juxtaposition (Massom et al.,

2013; Schemm, 2018). Different regions and seasons contribute to the total trend, which has made it difficult to establish clear drivers on a pan-Antarctic scale and suggests that no single mechanism can explain the variability in Antarctic sea ice (Stroeve et al., 2016).

There is currently no consensus on the primary mechanisms controlling this variability, and recent comprehensive reviews have articulated the complexity of the ocean-ice-atmosphere system in the Southern Hemisphere (SH; Hobbs et al., 2016; J. M. Jones et al., 2016). Surface winds play an important role, and changes in the ice edge have been linked to trends in wind-driven ice drift due to large-scale intensification in surface winds associated with the circumpolar lows around Antarctica (Holland & Kwok, 2012; Matear et al., 2015; Turner et al., 2013). Other studies suggest that ocean-ice feedback processes (Zhang, 2007) and ocean change (Jacobs & Comiso, 1997), such as Atlantic warming (Li et al., 2014) also play a part. Natural multidecadal variability of the atmosphere-ocean-sea ice system is another significant consideration (Mahlstein et al., 2013; Polvani & Smith, 2013). While these studies have helped to improve our understanding of how the ice, ocean, and atmosphere interact, further work is still needed to be able to interpret the mechanisms driving this dynamic and interactive system.

In both the Arctic and the Southern Ocean there is a pronounced annual cycle in the waxing and waning of sea ice, but the patterns of sea ice formation and melt are quite distinct in each hemisphere. Arctic SIE exhibits approximately symmetric melt and growth seasons; if anything, the average annual Arctic ice growth rate is slightly faster than its rate of retreat (Walsh & Johnson, 1979). On the other hand, the Antarctic has an asymmetric seasonal cycle characterized by a slow autumn advance (March to early September) and a rapid spring retreat (November to early February), where the spring retreat is nearly twice as fast as the autumn advance (Gordon, 1981). This contrast in ice growth and melt rates between hemispheres indicates fundamental differences between Arctic and Antarctic sea ice processes.

A key difference between the polar regions is their geography. The Arctic is an ocean surrounded by continents that constrain the sea ice in all but some of the peripheral seas (Eisenman, 2010; Maksym, 2019). Sea ice can extend from the North Pole to a latitude of 44°N along the northeast coastlines of North America and Asia, but most sea ice is found north of 70°N. Arctic summer ice has decreased particularly rapidly over the satellite record (Stroeve & Notz, 2018). On the other hand, Antarctica is a continent surrounded by oceans, and the growth of sea ice is not constrained by land at the northern boundary but instead is exposed to some of the planet's highest winds and waves. Multiyear sea ice is relatively rare in the Southern Ocean. Instead, sea ice fringes the continent during austral summer (at approximately 75°S) but reaches 55°S at its greatest winter extent, where it is limited principally by the Antarctic Circumpolar Current (ACC). The ACC presents a northern boundary that isolates the statically stable cold, fresh surface polar waters required for sea ice formation from the warmer subtropical surface waters (Martinson, 2012). As a result of interactions between wind, sea ice, solar radiation, and the ocean mixed layer (Gordon, 1981; Watkins & Simmonds, 1999), we observe an extensive seasonal cycle in Antarctica that dominates the global signal: Each year approximately 15×10^6 km² of ice forms and subsequently melts, compared to approximately 9×10^6 km² in the Arctic. A number of studies have examined different components contributing to the growth-melt asymmetry in the seasonal sea ice cycle in Antarctica. However, a full description of the mechanisms behind this phenomenon remains elusive. In this review we bring together these components to provide a conceptual model of the mechanisms that modulate the slow growth and fast melt in Antarctic SIE.

The sea ice and atmospheric reanalysis data used to illustrate the processes and concepts described in this review are briefly outlined in section 2. In sections 3 and 4 we review our current understanding of the trends and drivers of Antarctic SIE. The modest increasing trend, observed over the last four decades, masks substantial regional and seasonal changes. Evidence from proxies and historical records suggests that SIE has decreased over longer time scales, but further work is needed to understand the long-term changes with respect to internal variability. Despite the complex ice-ocean-atmosphere interactions that drive variability of the position of the ice edge, the asymmetric pattern in the annual freezing and melting of Antarctic sea ice remains remarkably consistent. In every year of the satellite record, Antarctic sea ice has a faster retreat season compared to the growth period, whereas the annual cycle is much more symmetric in the Arctic. In section 5 we compare and contrast these distinct annual cycles, averaged over the 40-year satellite record and highlight some interesting similarities and differences between the Northern Hemisphere (NH) and SH. In section 6 we discuss how well current climate models represent the characteristic asymmetric Antarctic seasonal cycle. Reproduction of the regular seasonal cycle is regarded as an important indication that the

model captures the rudiments of the system. A number of previous studies have explored the individual mechanisms responsible for this asymmetric pattern in Antarctic sea ice. However, a unified description of the phenomenon is still absent. In section 7 we tie together the various studies describing and explaining these mechanisms to provide a more complete picture of the annual cycle of sea ice around Antarctica. Finally, in section 8 we summarize the findings and provide a full description of the annual cycle of Antarctic sea ice.

2. Data Description

The Antarctic sea ice edge is rarely a distinct feature and instead can be diffuse over many tens of kilometers, which can make it difficult to determine the location of the ice edge accurately. The long-term (40-year) record of SIE relies on cloud-penetrating passive microwave retrievals that allow year-round observations. Limitations of this long-term product include the relatively coarse resolution (12–25 km), the fact that the measurement period spans a number of instruments with often short overlap periods between sensors (Meier et al., 2011), and the widespread use of a variety of different sea ice algorithms of varying strengths and weaknesses (Comiso & Nishio, 2008; Ivanova et al., 2015; Markus & Cavalieri, 2000). Differences between the algorithms are slightly higher during the summer months when challenging conditions such as thin ice and surface water from flooding are most common (Hobbs et al., 2016). While these algorithms do not always agree with each other in terms of absolute magnitude of SIE, the calculated trends and interannual variability are in general agreement (Comiso et al., 2017) and are therefore considered fairly robust when using a consistent data set.

Here, we use the National Snow and Ice Data Center (NSIDC) daily sea ice index version 3 (Fetterer et al., 2017), which is derived from Nimbus-7 SMMR and DMSP SSM/I passive microwave sea ice concentrations, to illustrate the annual cycles of Arctic and Antarctic sea ice. Daily SIE (1979 to present), as well as a climatological daily SIE (averaged over 1981–2010), are available from NSIDC. We calculated the climatological monthly mean latitude of the Antarctic sea ice edge from the 15% contour line in the National Oceanic and Atmospheric Administration/NSIDC Climate Data Record of monthly sea ice concentration (Fetterer et al., 2017), available for 1979–2016 at 25-km \times 25-km spatial resolution. The Climate Data Record comprises data from the NASA Team algorithm (Cavalieri and Parkinson, 2008) and the Bootstrap algorithm (Comiso, 1986), as well as a merged data set. We used the merged product as each algorithm has different advantages and disadvantages, with no clear winner: The Bootstrap algorithm performs better than the NASA Team algorithm around Antarctica and in the middle of the ice pack due to the dominance of snow-covered thick ice (Comiso & Steffen, 2001).

Meteorological observations are sparse in the Southern Ocean, so reanalysis data sets are needed to examine the long-term changes in atmospheric variables. The underestimation of wind intensity is a known general issue for reanalyses (R. W. Jones et al., 2016), but studies that have evaluated reanalysis data sets using surface and upper-level observations in Antarctica have found European Centre for Medium-Range Weather Forecasts (ECMWF) Re-Analysis (ERA)-Interim to be a fairly reliable analysis over the Southern Ocean (Bracegirdle & Marshall, 2012; Bromwich et al., 2011). Data for the mean sea level pressure over the Southern Ocean and Antarctic Continent, used to calculate the semiannual oscillation (SAO) Index and the location of the Antarctic Circumpolar Trough (CPT), come from the ERA-Interim monthly fields from 1979–2016 (Dee et al., 2011), as do the 2-m air temperatures for estimating regions of potential freezing. We derived climatological monthly means of sea level pressure from the ERA-Interim monthly fields and calculated the SAO Index following the method described in Meehl et al. (1998). We identified the monthly mean location of the circumpolar trough by calculating the mean latitude of the climatological minimum pressure for each month.

3. Trends in Antarctic SIE

Sea ice change and variability are often described in terms of SIE, which is the integral sum of all grid cells with a sea ice concentration greater than some threshold value (typically 15%). Sea ice area (SIA), determined by taking the sum of the product of the area and the ice concentration of each grid cell, is another useful metric from which ice volume and ice mass can be derived. In practice the metrics are highly correlated; the two mainly differ in that SIA excludes regions of open water within the ice pack. SIE is more commonly

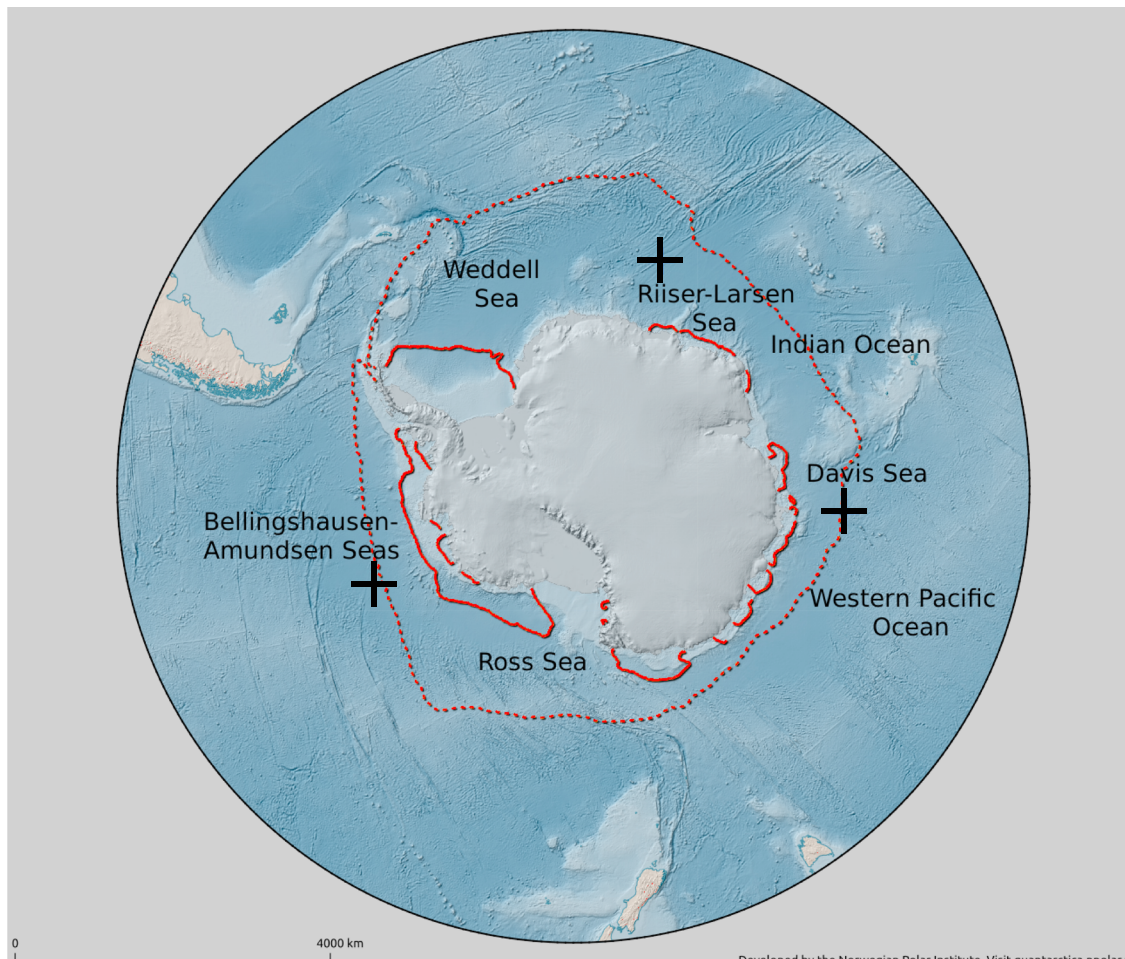


Figure 1. Geography of the Southern Ocean and the locations of regions and sectors often chosen to examine trends and variability. The solid red line shows the minimum sea ice extent, and the dashed red line shows the maximum sea ice extent (both median values for 1981–2010). The black crosses show the approximate mean locations of the three climatological low-pressure systems.

cited because uncertainties in passive microwave retrievals have less effect on SIE (Hobbs et al., 2016). The average Antarctic SIE ranges from a summer minimum of 3.1×10^6 km² in February, when isolated pockets of consolidated sea ice fringe the continent, to a winter maximum of 18.5×10^6 km² in September (Parkinson, 2014). The winter sea ice extends over an area roughly the size of the continent itself (Figure 1). Despite its vast extent, Antarctic sea ice forms only a thin veneer on the ocean's surface, less than 1 m thick on average (Worby et al., 2008). Although most sea ice in Antarctica is seasonal, freezing in winter and melting again each summer, in a few coastal regions the sea ice remains all year round (Figure 1). On average, the autumn ice edge advance takes about 7 months to progress from near the coast in February (the solid red line on Figure 1) to its September most northward maximum (the dashed red line on Figure 1) and about 5 months to return to its February minimum.

3.1. Trends in Total SIE Over the Last 40 Years

The annual sixfold change in the Southern Ocean sea ice cover has been routinely monitored since the advent of satellite passive microwave imagery, 40 years ago. A modest hemisphere-wide increase of $1.6 \pm 0.4\%$ per decade has been observed over 1979–2016 (Comiso et al., 2017; de Santis et al., 2017), but extreme changes have occurred in recent years, with record winter maxima recorded in 2012, 2013, and 2014 (Massonnet et al., 2015), followed by record summertime minima in 2017 and 2018 (Meehl et al., 2019; Turner et al., 2017). However, this overall, increasing trend runs counter to the projections of most climate models (Turner et al., 2015) and a decrease in Antarctic SIE is projected by 2100 in all of the representative concentration pathways (RCPs) examined by the Intergovernmental Panel on Climate Changes Fifth Assessment Report (Collins et al., 2013).

There has been much interest in the Antarctic trends since they are opposite to what is expected under globally warming surface temperatures. Drivers of change in Antarctic sea ice are discussed in more detail in section 4, but it is worth summarizing recent work on the increasing trend (1979–2016) and the recent record low sea ice cover (2016–2018). Antarctic sea ice is not bounded by land and is free to vary in response to atmospheric and/or oceanic influences. Suggested drivers of the weak positive Antarctic SIE trend include internal variability (Mahlstein et al., 2013; Polvani & Smith, 2013), cooling of the Southern Ocean surface due to the observed strengthening of the westerly winds and positive trend in the Southern Annular Mode (SAM) resulting from ozone depletion (Ferreira et al., 2015), teleconnection patterns driven from various areas in the tropics and associated surface wind anomalies at high southern latitudes (Ciasto et al., 2015; Clem & Fogt, 2015; Ding & Steig, 2013; Hobbs et al., 2015; Li et al., 2014; Simpkins et al., 2014), and ice sheet meltwater (Bronse laer et al., 2018). However, there is still no consensus on the cause of the upward trend and this remains a puzzle. Comiso et al. (2017) found the positive trend in sea ice cover to be strongly correlated with the trend in surface temperature and suggested that better representation of surface temperatures in climate models is needed to ensure better agreement with the observed trend.

After nearly four decades (1979–2016) of observed increasing trends of Antarctic SIE, there has been a dramatic decrease in recent years (2016–2018). The decay was particularly strong in November 2016, when Antarctic SIE exhibited a negative anomaly compared to the 1979–2015 average (Schlosser et al., 2018). Several studies have investigated the possible factors driving this recent decline and found it to be linked to a warmer upper Southern Ocean (Meehl et al., 2019), to an anomalous atmospheric circulation with an amplified zonal wave 3 pattern (Schlosser et al., 2018; Wang et al., 2019) and to a significantly weakened polar stratospheric vortex, resulting in record weakening of the circumpolar surface westerlies that acted to decrease SIE (Wang et al., 2019).

3.2. Long-Term Trends From Historical and Proxy Sources

The observed positive trend is small and the recent record lows in observed SIE suggest that it was potentially short-lived. Forty years is insufficient to accurately assess the multidecadal variability and long-term trends of the system (Goosse et al., 2009), especially with the high internal variability of the Southern Ocean climate system. Proxy records can give some context for multidecadal to multimillennial time scales, albeit with large associated uncertainties. Efforts have been made to extend the record of SIE using approaches based on biogenic or geochemical proxies derived from marine sediments, ice cores and coastal records de Vernal et al. (2013). For example, methane sulphonic acid sources in ice cores are related to marine phytoplankton productivity, which is strongly modified by sea ice processes at the ice margin. Methane sulphonic acid has been shown to give a reliable estimate of regional sea ice cover on interannual time scales (Abram et al., 2013). In addition, historical records from whale catch locations (de la Mare, 2009) and observations of the summer ice edge from ship logbooks from the “Heroic Age” of Antarctic exploration (Edinburgh & Day, 2016) have been used to estimate SIE from the late nineteenth century onward. Early satellite missions have also provided snapshot estimates of SIE since 1964 (Meier et al., 2013). However, the ability of these proxy and historical records to quantitatively estimate changes in SIE has been questioned Ackley et al. (2003); Ozsoy-Cicek et al. (2009). For example, Ozsoy-Cicek et al. (2009) showed that the bias between the definition of the ice edge derived from ship logs compared to that derived from satellite data could be more than 10^6 km² during some seasons. Care must clearly be taken in comparing proxy and historical records with modern satellite observations, but as the only available information on longer time scales, these records comprise a valuable data set for putting recent changes in SIE into a longer-term context.

3.3. Regional and Seasonal Trends in Antarctic SIE

The marginal increase in total Antarctic sea ice over the last four decades masks substantial regional trends of increasing ice extent, primarily in the Ross and Weddell Seas, and decreasing ice extent in the Bellingshausen and Amundsen Seas (Table 1). This dipole pattern of change is the most marked observed trend. There are complex spatial patterns of change in advance, retreat and duration and it can be hoped that examining the individual regions can help us understand the overall trends.

From a seasonal perspective, autumn and summer have the largest trends and spring the lowest (Figure 2 and Table 2). In all regions the trends grow in spring, resulting in the maximum trends in the summer, which decay in autumn, and no significant trend is seen in the winter sea ice concentrations (Holland, 2014). Seasonal descriptions of change are also complicated by the fact that most analyses use traditional seasons, for example, summer (December–January–February) and winter (June–July–August), while key seasons for

Table 1
Annual Regional Trends in Antarctic Sea Ice Extent (Percent Change per Decade)

Sector	de Santis et al. (2017) ^a	Comiso et al. (2017) ^b	Maksym (2019) ^c
Total	1.6 ± 0.4	1.73 ± 0.34	1.0
Indian Ocean	1.7 ± 0.9		1.2
Ross Sea	3.3 ± 0.9		2.4
Weddell Sea	1.7 ± 0.8		1.2
Western Pacific Ocean	1.8 ± 1.2		2.0
Bellingshausen-Amundsen Seas	-2.9 ± 1.4		-3.1

Note. Figure 1 provides the geographic setting of the named sectors.

^a 1979–2016. ^b 1979–2015. ^c 1979–2017.

sea ice are the periods of advance and retreat (Raphael & Hobbs, 2014; Renwick et al., 2012; Stammerjohn et al., 2008). These do not exactly coincide with the atmospheric seasons. Nonetheless, previous studies have found contrasting changes in sea ice seasonality in the north-east and west Antarctic Peninsula and southern Bellingshausen Sea and western Ross Sea regions (Jacobs & Comiso, 1997; Stammerjohn et al., 2008).

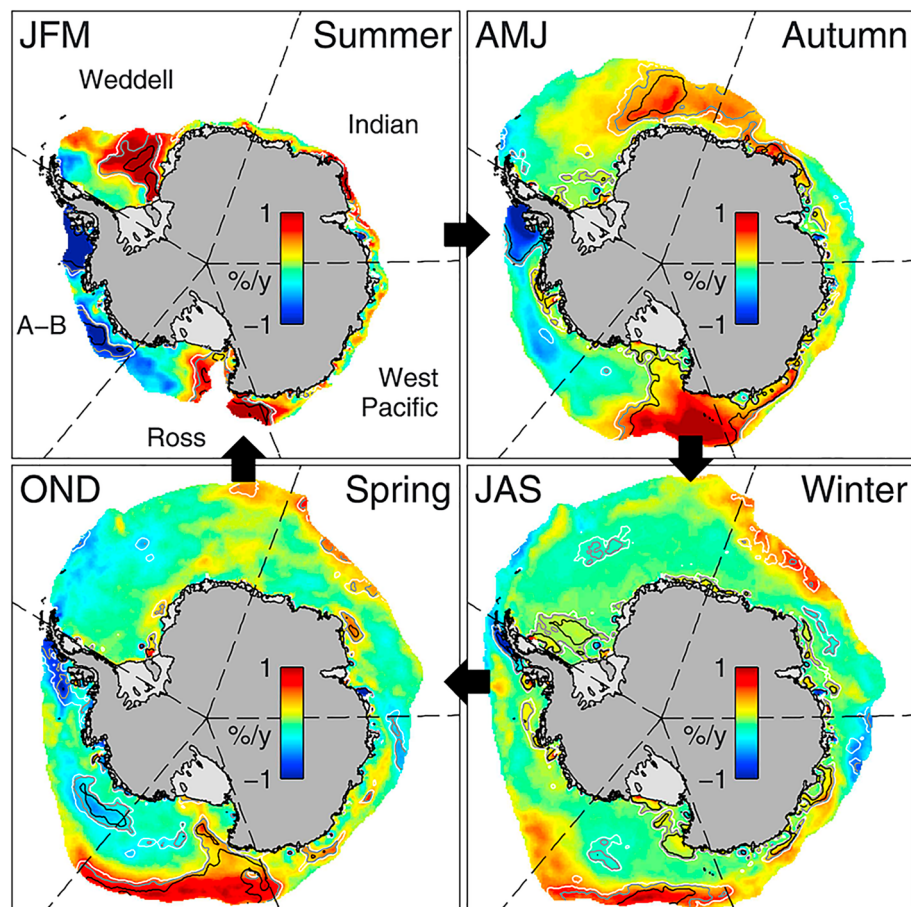


Figure 2. Map of seasonal trend in sea ice concentration from Holland (2014). White, gray, and black contours show 90%, 95%, and 99% significance, respectively. Reproduced with permission from John Wiley and Sons. JFM = January-February-March; AMJ = April-May-June; JAS = July-August-September; OND = October-November-December.

Table 2
Seasonal Trends in Antarctic Sea Ice Extent (Percent Change per Decade)

Season	Comiso et al. (2017) ^a
Annual	1.73 ± 0.34
Winter	1.39 ± 0.32
Spring	0.93 ± 0.27
Summer	2.54 ± 1.10
Autumn	3.79 ± 1.05

^a 1979–2015.

3.4. Trends in Sea Ice Duration

Timing and duration of sea ice cover are crucially important for the structure and dynamics of Southern Ocean marine ecosystems (Massom et al., 2013) and have an important feedback with the upper ocean: earlier spring ice melt results in increased ice production in autumn, later melt leads to decreased autumn production (Stammerjohn et al., 2012). Figure 3 shows the climatological mean number of ice days per year (1979–2017). The trends in sea ice duration follow the same spatial pattern as the trends in SIE. In particular, the annual ice-free period has shortened by 2.6 months in the western Ross Sea due to an earlier advance and later retreat, but has increased by 3.3 months in the Bellingshausen Sea, mostly due to a later advance (Hobbs et al., 2016).

Finally, it is worth noting that volumetric changes, unlike areal changes, are not adequately captured with existing satellite technology. Sea ice thickness is a key measure of sea ice volume and longevity but a reliable estimate of even the average ice thickness and that of its snow cover still eludes us (Giles et al., 2008). Uncertainties in the degree of radar penetration into the snow pack has so far limited the use of the radar altimeter record for measuring sea ice thickness. There is no large-scale, long-term record of sea ice thickness for Antarctica and therefore little is known about how the total mass of the sea ice cover has changed in time. This remains a significant gap in Southern Ocean observations.

4. Main Drivers of Trends in Antarctic SIE

The overall positive trend in Antarctic sea ice is not well reproduced in climate models (Turner et al., 2013), with most producing a decreasing trend (section 6). However, it has been shown that the small number of Coupled Model Intercomparison Project Phase 5 (CMIP5) models that correctly simulate the negative phase of the Interdecadal Pacific Oscillation (IPO) do have an increasing trend in SIE (Meehl et al., 2014, 2016). Turner et al. (2012) suggested that the trend does seem to be within the bounds of natural climate variability.

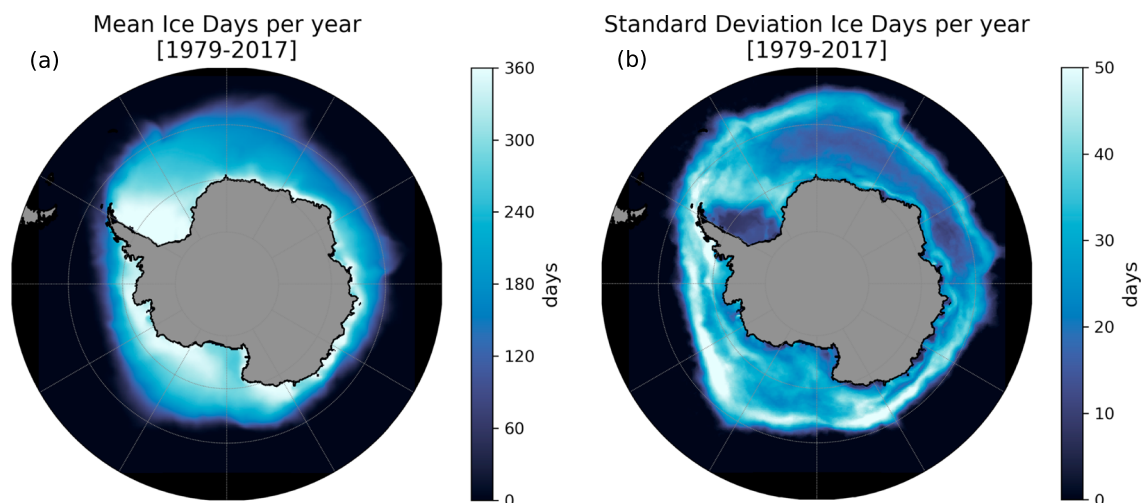


Figure 3. (a) Climatological mean number of ice days per year for the period 1979–2017. (b) Standard deviation. In both figures the data set used is the merged product from the National Oceanic and Atmospheric Administration/National Snow and Ice Data Center Climate DATA Record of daily sea ice concentration (Fetterer et al., 2017).

Potential driving mechanisms underlying these changes include changes in surface temperature (Comiso et al., 2017), wind direction (Hobbs et al., 2016; Holland & Kwok, 2012; Massom et al., 2008; Mayewski et al., 2009; Stammerjohn et al., 2003; Turner et al., 2016), sea ice drift (Pope et al., 2017), precipitation (Liu & Curry, 2010), ice-ocean feedbacks (Goosse & Zunz, 2014), changes in the entrainment of warm deep water into the winter mixed layer (Zhang, 2007), and meltwater from the Antarctic ice sheet (Bronse laer et al., 2018). It is known that sea ice responds to many different interactive processes in the atmosphere and ocean (Hobbs et al., 2016). These include the advection of heat, the horizontal movement of sea ice by wind and ocean currents and meltwater from icebergs, ice shelves and marine-terminating glaciers. In this section, we give an overview of the main processes and their possible role in driving the observed trends in SIE described in section 3.

4.1. Atmospheric Drivers

The atmosphere plays a vital role in modulating Antarctic SIE. Surface winds are considered to be the chief dynamic agent underlying sea ice variability, and they explain most of the observed interannual variability and much of the trends (Holland & Kwok, 2012; Kwok et al., 2017; Matear et al., 2015; Schemm, 2018). The surface winds that drive sea ice motion and variability around Antarctica are strongly linked to weather systems, which in turn are the result of the larger scale climate variability.

4.1.1. Drivers at the Regional Scale: Weather Systems

Synoptic-scale circulation is an intermediate scale that connects the hemisphere-wide modes of SH climate with the 10-m wind circulation, which is at the origin of regional-scale sea ice trends (Hobbs et al., 2016; Schemm, 2018; Turner et al., 2016). Changes in storm track activity and location are thought to be a significant forcing factor in the observed sea ice trends, and there is a marked correlated tendency toward fewer but more intense cyclones in the sea ice zone (Simmonds et al., 2003). However, pinpointing the origin of changes in regional SIE is complex since anomalies can result from accumulated rates of change of sea ice concentration, also referred to as “intensification” by Holland (2014), during the preceding seasons (Holland, 2014; Schemm, 2018). For example, Holland (2014) noted that in some regions, springtime intensification rates can drive SIA anomalies during the following autumn. Furthermore, Holland, Landrum, Raphael, and Stammerjohn, et al. (2017) found that the western Ross Sea SIE in autumn is inversely correlated with the 10-m zonal wind speed anomalies during the preceding spring, which are, in turn, related to weather system anomalies. Schemm (2018) discovered that regions with strong trends in SIE during spring and autumn have strong, accompanying trends in the number of days they are affected by either a low-pressure system or a stationary, high-pressure system (atmospheric block).

There are three climatological low-pressure systems within the Antarctic circumpolar trough, centered over the Amundsen, Riiser-Larsen, and Davis Seas, and their approximate locations are shown by the blue crosses in Figure 1. Kwok et al. (2017) found that the location and depth of these lows control three spatially distinct sea ice drift patterns and is also linked to the interannual variability in ice export in the Ross and Weddell Seas. They also demonstrated that seasonal trends in ice edge are linked to trends in meridional winds and also to on-ice/off-ice trends in zonal winds, due to the zonal asymmetry of the Antarctic ice cover. On average two thirds of the winter ice edge trend in the Pacific sector can be explained by changes in meridional winds and associated ice drift, linked to extratropical atmospheric anomalies associated with the Southern Oscillation, which can be translated locally to changes in the atmospheric low over the Amundsen Sea (Kwok et al., 2016).

The Amundsen Sea Low (ASL; Hosking et al., 2013; Raphael et al., 2016; Turner et al., 2013, 2016) stands out as an important feature of the circumpolar atmosphere's meridional flow around Antarctica. It is a quasi-stationary atmospheric low-pressure anomaly at approximately 60–70°S, with a climatological mean zonal location that shifts from 220°E in winter to 250°E in summer (Hosking et al., 2013). It occurs as a result of zonal flow around the continental topography (Baines & Fraedrich, 1989) and is therefore closely related to the SAM (Lefebvre et al., 2004; Turner et al., 2013), a measure of the position and intensity of the westerly winds that circle Antarctica. Cyclonic flow around the ASL drives warm, poleward winds into the Antarctic Peninsula/Bellingshausen Sea region and a cold equatorward wind over the Ross Sea, which is thought to contribute to the dipole in sea ice trends between these two regions (Holland & Kwok, 2012; Hosking et al., 2013; Lefebvre et al., 2004; Turner et al., 2015, 2016). The deepening of the ASL has been a focus of recent research, and indeed, this deepening is consistent with some of the observed sea ice trends, in particular, the loss of ice and warming of the Bellingshausen Sea, and an increase in some seasons in the eastern Ross Sea. However, its relationship to increased ice coverage in the western Ross Sea is not well understood Hobbs

et al. (2016). Kusahara et al. (2018) found that sea ice variability in West Antarctica is strongly linked with the activity of the ASL.

4.1.2. SH Climate Variability

Several studies have focused on exploring the connections between the heterogeneous Antarctic sea ice trends and various climate , such as the SAM, the El Niño–Southern Oscillation (ENSO), and the IPO detailed below (Hobbs et al., 2016; Kwok et al., 2016; Lefebvre et al., 2004; Pezza et al., 2012; Stammerjohn et al., 2003, 2008), and on the role of seasonal feedbacks (Holland, 2014; Holland, Landrum, Raphael, et al., 2017). So far, no consensus has been reached on how climate modes affect the changes in Antarctic sea ice.

On the hemispheric scale, the SAM, a periodic equator-to-pole shift of the circumpolar-veering westerly jet stream, is affected by a long-term trend toward more poleward contracted westerlies (Marshall, 2003; Thompson & Solomon, 2002). Kwok et al. (2017) have shown that anomalies in large-scale ice conditions around Antarctica are linked to the variability in the Southern Oscillation and the SAM. Hobbs et al. (2015, 2016) summarized the potential impact of these major modes for the observed SIE trends and concluded that tropical teleconnections explain little of the trends in any season. The positive SAM trend has its biggest impact in summer and may explain some of the decrease in SIE in the Bellingshausen Sea, but the signal is contrary to observed trends in the Amundsen and Weddell seas. Additionally, contrasting SIE conditions have occurred recently with record high in 2014 and record low in 2016 both under a strongly positive SAM (Meehl et al., 2016, 2019). The role of the SAM in modulating the SIE interannual variability needs to be further investigated, together with links to the zonal wave 3 pattern (Schlosser et al., 2018) and the variability in the tropics.

Antarctic sea ice also has a strong response to tropical sea surface temperature (SST) anomalies via the ENSO (Gloersen, 1995; Simmonds & Jacka, 1995; Simpkins et al., 2013; Turner, 2004; Yuan, 2004). Atmospheric anomalies excited by tropical Pacific convection propagate southeastward by way of an atmospheric Rossby wave train to the high-latitude southeastern Pacific (Yu et al., 2011), a mode commonly referred to as the Pacific South American mode (Karoly, 1989; Mo, 2000; Mo & Higgins, 1998; Mo & Paegle, 2001). The response is most evident in the eastern Ross and Amundsen-Bellingshausen Sea sectors (Gloersen, 1995; Simmonds & Jacka, 1995; Turner, 2004; Yuan, 2004), and peaks during the late austral winter and spring (Jin & Kirtman, 2009; Mo & Higgins, 1998; Simpkins et al., 2013). During warm ENSO events (i.e., El Niños), a high-pressure anomaly is set up, centered at approximately 90°W, 55°S, and this weakens the ASL (Turner, 2004; Yuan, 2004; Yuan & Li, 2008). There is a notable asymmetry between the responses to warm and cold ENSO events (Houseago-Stokes & Mcgregor, 2000; Simpkins et al., 2013; Yuan, 2004), and the strength of the high-latitude SH teleconnection is highly variable. While the fickleness of the teleconnection has been attributed to internal variability (Sterl et al., 2007), there is evidence that the response to ENSO is modulated by the background state of the SAM. The ENSO teleconnection is only statistically significant when SAM is in a weak (i.e., neutral) phase, or when SAM is in phase with the driving ENSO event. That is to say that the teleconnection with El Niño is significant when the SAM is in a negative phase, and with La Niña when the SAM is in a positive phase (Fogt & Bromwich, 2006; Fogt et al., 2011; Stammerjohn et al., 2008). Observation-based studies have shown that, although important for interannual variability, ENSO contributes little to the overall trends in Antarctic sea ice (Kohyama & Hartmann, 2016; Simpkins et al., 2013; Yu et al., 2011) and that currently there is no widely established mechanism that links tropical Pacific SST anomalies to the SAM (Ciaсто et al., 2015).

However, it has been suggested that West Antarctic surface temperature changes may be related to Multidecadal modes of Pacific variability (Ding et al., 2011; Okumura et al., 2012; Schneider & Steig, 2008). Meehl et al. (2016) showed that the largest (up to 75%) IPO contributions to the twentieth-century global surface temperature trends, including Antarctica surface temperatures, occurred in its positive phase during the rapid warming periods from 1910–1941 and 1971–1995. Ding and Steig (2013) have examined the link between the tropical Pacific and the temperature change on the Antarctic Peninsula and found that the most important large-scale forcing of the significant widespread warming trend in fall is the extratropical Rossby wave train associated with tropical Pacific SST anomalies. Clem and Fogt (2015) found that after 1979, statistically significant warming in Antarctica is only observed in austral spring across West Antarctica and the Antarctic Peninsula and that a substantial (30–60%) portion of the warming is related to changes in the spring atmospheric circulation. In particular, western Antarctic Peninsula warming is consistent with increasing pressure in the South Atlantic associated with a trend toward more La Niña-like conditions in the tropical Pacific, and an associated Rossby wave train. Whereas western West Antarctica warming is tied

to a deepening of the ASL near the eastern Ross Sea which is strongly associated with a shift in the Pacific Decadal Oscillation toward its negative phase since the 1990s.

There is also a possible link between multidecadal tropical Atlantic variability and West Antarctic sea ice (Li et al., 2014; Simpkins et al., 2014), with a physical mechanism that is similar to the tropical Pacific teleconnection, where precipitation and convective heating associated with tropical SSTs anomalies drive anomalous Rossby wave and teleconnections to higher latitudes. Under warming tropical Atlantic conditions (as has been the case since 1979), the ASL tends to deepen, driving Bellingshausen and eastern Ross sea ice changes in winter (Li et al., 2014) and spring (Simpkins et al., 2014). Hobbs et al. (2015) found that removing the linear signal of the Atlantic Multidecadal Oscillation and IPO indices from Antarctic SIE had some impact on the observed trends in those seasons, but not enough to explain the full Ross Sea trend. Teleconnections with multidecadal tropical Pacific and Atlantic variability in SST have been suggested as a contributing factor, but the magnitude of their influence on trends is not well-established; an initial analysis presented by Hobbs et al. (2016) indicated that it may be modest.

In summary, the major modes of SH atmospheric variability likely play an important role in defining the interannual variability of Antarctic sea ice. However, despite numerous studies considering the regional impact of atmospheric changes on Antarctic sea ice coverage, it has so far not been possible to explain the observed sea ice trends solely by trends in these major modes. This is especially true of the Ross Sea sector, which contributes most of the observed increase in total SIE since 1979 (Parkinson & Cavalieri, 2012).

Changes in the atmospheric modes described above lead to pronounced changes in wind stress and thermodynamic forcing. Kushara et al. (2018) used an ocean-sea ice model to examine the response of Antarctic sea ice variability fields to the physical mechanisms of wind stress and thermodynamic surface forcing. They showed that sea ice response to wind stress and thermodynamic forcing differ according to season and region. Thermodynamic forcing is the main driver of sea ice variability during autumn and winter, while wind stress plays a dominant during the summer. In the melt season, both effects are comparably important in driving variability of the total SIE. However, there are also regional variations in the response with variability of the sea ice edge in the Ross Sea mainly controlled by wind stress, whereas thermodynamic forcing plays a strong role in other regions.

4.1.3. Ocean and Ice Sheet Melt Drivers

Although the atmosphere likely plays a dominant role in controlling the Antarctic sea ice interannual variability, the ocean is also believed to play an important role. So far there is no robust evidence that the ocean is a primary driver of sea ice, but atmospheric forcing can have an important two-time scale response in the Southern Ocean (Ferreira et al., 2015; Holland, Landrum, Kostov, et al., 2017; Kostov et al., 2017). For example, sustained westerlies lead to increased Ekman drift and therefore increased Antarctic SIE due to direct wind forcing and colder SSTs in the short term, but the enhanced upwelling can bring warmer subsurface water to the surface, contributing to reduced growth and/or enhanced melt in the longer term. Meehl et al. (2019) attributed part of this two-time scale response to the recent rapid decrease in Antarctic sea ice that began in 2016, where one of the main contributing factors was a decadal time scale trend of negative wind stress curl anomalies over the 2000s, associated with the positive trend of the SAM and the negative phase of the IPO led to upwelling of warmer subsurface water. Due to sparse observations, much of the research into the role of the ocean relies on modeling studies in which the Southern Ocean is often still poorly constrained (Russell et al., 2006).

The ACC sets the northern limit for sea ice formation by separating the cold fresh surface polar waters from the warm subtropical surface waters (Martinson, 2012). A series of sub-polar gyres lie poleward of the ACC, most notably the Weddell Sea and the Ross Sea Gyres. These gyres lie within the winter sea ice cover. Climatological patterns of sea ice drift around Antarctica also reflect the climatological ocean surface current patterns, but these in turn are largely wind-driven (Hobbs et al., 2016). The Ross Sea Gyre is associated with the ASL and the associated sea ice drift pattern shows a coastal inflow of sea ice into the Ross Sea that moves southward along the coast, with a strong northward outflow in the west. (Kwok et al., 2017). The Weddell gyre is associated with the Riiser-Larsen Sea Low drift pattern, a cyclonic drift pattern that dominates the ice drift March through November (Kwok et al., 2017).

The vertical structure of the near-surface water column is highly seasonal in the sea ice zone due to heat and salt fluxes related to ice formation and melting. Figure 4 shows a highly simplified conceptual model of the seasonal change in the vertical structure of the ocean between the winter freezing period and the spring

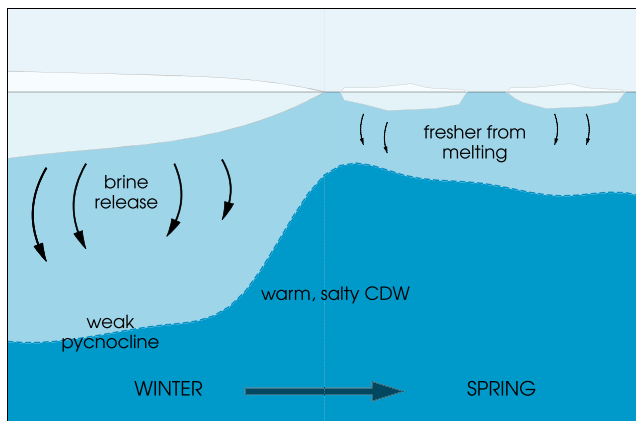


Figure 4. Schematic representation of the variation of mixed layer depth and stabilization of the Southern Ocean through winter and spring by sea ice processes. CDW = Circumpolar Deep Water.

melting season. The general structure of the Southern Ocean comprises a cool, fresh mixed layer floating on the relatively warm and salty Circumpolar Deep Water (CDW). Brine rejection during autumn freezing drives vertical mixing that entrains the warmer water below into the mixed layer (Martinson, 1990), which is thought to provide a thermal limit to the seasonal ice thickness. Ocean stratification and the presence of sea ice are therefore tightly linked, and both positive and negative feedbacks have been described. Zhang (2007) found a negative feedback where *reduced* sea ice growth during autumn led to a decrease in brine rejection and a subsequent increase in ocean stratification. Consequently, less warm water is brought to the ocean surface and there is less spring melt. However, Goosse et al. (2009) and Goosse and Zunz (2014) described a positive feedback in which *increased* ice coverage leads to a much fresher surface layer during the spring melting season, which also increases stratification, subsequently leading to reduced melting. Most of the Antarctic sea ice cover melts entirely in the summer, so this may not make much difference over the course of a single annual cycle. However, there can be a net freshening of the surface layer that persists for years to decades. Hobbs et al. (2016) also suggest that whether there is a positive or negative feed-

back depends on the background state of the water column, horizontal ice motion, and the time scales involved. However, there appears to be a spatial dependence on where these processes are important, and rigorously identifying where these feedbacks occur would be a significant advance in our understanding.

Sea ice-ocean feedbacks may be important in the transferral of sea ice anomalies from one season to the next (Holland, 2014; Stammerjohn et al., 2012), but these interactions and feedbacks are strongly dependent on region and season (Maksym et al., 2012). The timing of sea ice retreat seems to have a strong influence on the timing of the following advance, whereas advance and subsequent retreat are only weakly related (Stammerjohn et al., 2012), which suggests that a strong ocean thermal feedback accelerates or decelerates the onset of autumn freezing. Earlier wind-driven sea ice retreat can lead to upper-ocean warming and continued decreases in sea ice, resulting in a positive feedback (Meredith & King, 2005). This mechanism has been attributed to accelerated sea ice retreat in the Bellingshausen Sea. On the other hand, enhanced ice divergence under strengthening westerlies can lead to a negative feedback where increased ice production causes more convective overturning and upward heat flux to inhibit ice growth (Sigmond & Fyfe, 2010). Such feedback processes are critical for understanding the present and future behavior of Antarctic sea ice.

In coastal regions, ice-shelf melt also has the potential to affect sea ice through the influence of fresh water on the water column. Freshening by ice sheet meltwater can increase stratification, which has been shown to reduce SSTs and cause subsurface ocean warming (Fogwill et al., 2015; Park & Latif, 2018). There is also some evidence that meltwater can potentially increase SIE (Bintanja et al., 2013; Pauling et al., 2017). In a modeling study, Bronselaer et al. (2018) found evidence that by 2100 the influx of ice sheet meltwater may cause a substantial increase in annual mean SH SIA, which is dominated by winter anomalies.

4.1.4. Anthropogenic Forcing

It has been argued that there is a clear link between anthropogenic emissions and the recent decline of Arctic sea ice (Notz & Stroeve, 2016), but although Antarctic sea ice trends may well be forced by greenhouse gas emissions, it is currently not understood how the observed trends may be linked to human activities. There are a number of reasons why the detection of anthropogenic consequences is challenging in Antarctica: the observational record is relatively short; the response may be small compared to the high natural variability of the system; and coupled global climate models do not faithfully represent the complex Antarctic climate system (Hobbs et al., 2016). Some of the drivers of changes in Antarctic sea ice trends may also be influenced anthropogenically, in particular the winds and climate modes.

Holland and Kwok (2012) have argued that modern trends in the SAM and ENSO (and therefore wind and ice-motion trends) could arise through natural variability, but some evidence suggests that they are at least in part due to the SH ozone hole and increased greenhouse gases. Hobbs et al. (2016) showed that significant atmospheric trends have been observed over the same period as the sea ice trends and argue in particular for an anthropogenically forced shift toward a positive phase of the SAM, and an attendant increase in circumpolar westerlies over the Southern Ocean. It is not clear whether this would be expected to force

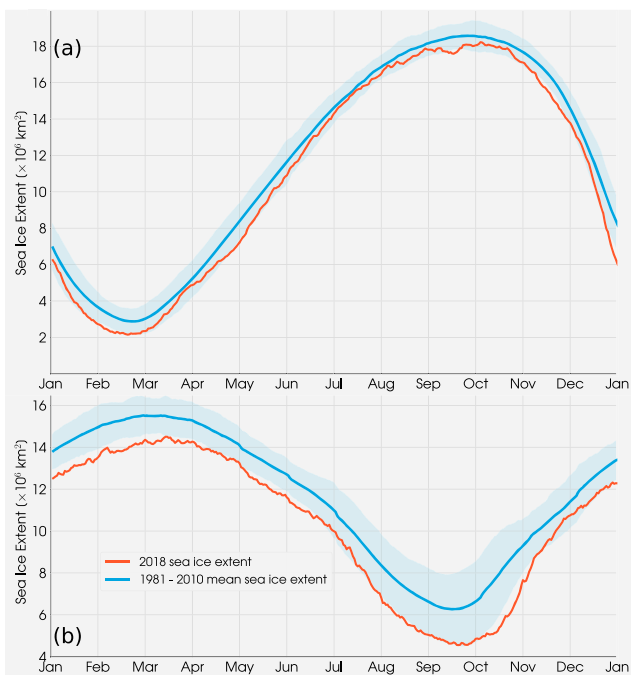


Figure 5. Seasonal cycle of (a) Antarctic sea ice extent and (b) Arctic sea ice extent for the duration of the satellite record (Fetterer et al., 2017). The blue line shows the 1981–2010 mean SIE, as provided by National Snow and Ice Data Center. The blue shading shows 2 standard deviations from the mean. The red line shows the SIE for 2018. SIE = sea ice extent.

record, there are more “growth days” than “melt days,” even though the interannual variation in mean SIE varies by nearly 3×10^6 km², and the timing of the ice edge advance and its subsequent retreat can vary significantly.

The pattern of the Arctic sea ice seasonal cycle has also remained consistent despite the well-publicized year-to-year decrease of SIE in recent years. The timing of melt onset and freeze-up of the sea ice cover show a clear trend of earlier melt and later freeze-up and an overall longer melt season (Stroeve et al., 2014), leading to slightly more days of melting rather than freezing (opposite to the Antarctic), but since 2000 this trend in increasing melt season has slowed, even though Arctic SIE has continued to decline. Overall the Arctic cycle is much more symmetric than the Antarctic signal, with a very slight asymmetry in the opposite direction of 6.5 months melt and 5.5 months growth, as first noted by Walsh and Johnson (1979).

For easier visual comparison, Figure 6 shows the normalized and time-shifted curves of annual SIE for both the Arctic and Antarctic. Overall, the growth period in the Arctic is 2 weeks shorter than the melt period (5.5 months vs. 6.5 months) and the growth period in Antarctica is 2 months longer than the melt period (7 months vs. 5 months). At both poles, there is a sluggish winter turn compared to the rapid summer turn; that is, in the Antarctic, SIE is greater than 99% of the maximum extent for 24 days compared to only 6 days at less than 1% of its minimum extent; in the Arctic SIE is more than 99% of the maximum extent for 20 days compared to just 2 days at less than 1% of the minimum extent. This difference between the summer minimum compared to the winter maximum in both hemispheres may in part be due to the fact that sea ice responds more quickly at warmer temperatures. The blue line in Figure 6a demonstrates clearly that the maximum rate of melting is approximately twice the maximum growth rate, as first noticed by Gordon (1981) and that these extraordinarily high rates of change occur over just a couple of months, whereas the maximum melt and growth rates are very similar for Arctic sea ice.

Note that this pattern of slow growth and fast melt is observed in the averaged cycle for the whole Antarctic sea ice region, but significant regional variations do occur. For example, Stammerjohn et al. (2003) showed that in the western Antarctic Peninsula region, the sea ice advance season was generally either shorter than

an increase or decrease in SIE over the three to four decades of observed trends, and observational studies suggest that the SAM trend explains only a part of the sea ice trend pattern. Detection and attribution studies rely on coupled climate model experiments. These will be discussed further in section 6.

5. Annual Cycles of Arctic and Antarctic Sea Ice

In section 3 we discussed the modest, positive trend in Antarctic SIE that has been observed in the satellite record. In this section we examine the seasonal cycle in Antarctic SIE and contrast it to that in Arctic SIE. The failure of climate models to capture the long-term behavior partly reflects a poor understanding of sea ice processes (Maksym et al., 2012). Sea ice is a key component in the climate system and the ability of the CMIP models to simulate its mean state is an important check on the model ability to represent the system. As discussed by Notz (2014) and Ivanova et al. (2016), model simulations with the same SIE could have very different sea ice cover characteristics. Nonetheless, reproduction of the annual cycle remains a fundamental part of sea ice dynamics and understanding processes involved with the seasonal cycle can provide insight into changes in sea ice on longer time scales.

Figure 5 shows the annual cycles and interannual variation of the Antarctic and Arctic SIE from the NSIDC daily sea ice index v3 (Fetterer et al., 2017). Slow growth and rapid melt characterize the Antarctic cycle, and this pattern is seen consistently throughout the satellite record, which is remarkable, considering the huge regional, seasonal and interannual variability of Antarctic sea ice observed over this period (Parkinson & Cavalieri, 2012; Raphael & Hobbs, 2014). For all years in the satellite

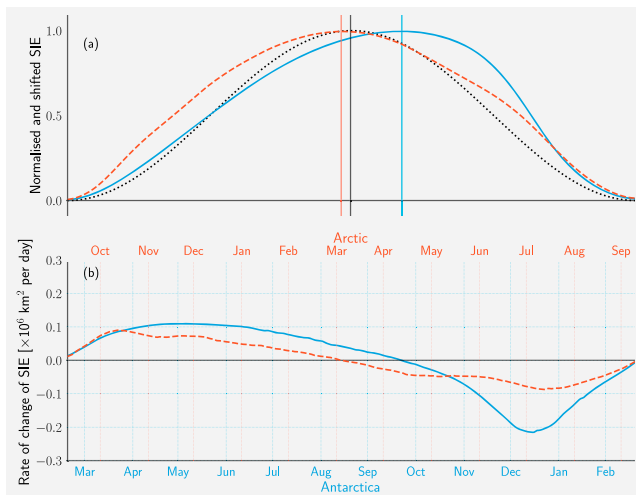


Figure 6. (a) The thick dashed lines compare normalized and shifted sea ice extent (solid blue is Antarctic, dashed red is Arctic, dotted black is a symmetrical curve). The vertical colored lines show the time of maximum sea ice extent at each pole (blue = Antarctic; red = Arctic, and black = maximum extent for a symmetrical cycle with equal growth and melt periods). The daily National Snow and Ice Data Center data have been smoothed with a 30-day running mean. (b) Rate of change of sea ice extent (solid blue is Antarctic, dashed red is Arctic). SIE = sea ice extent.

or equivalent to the period of sea ice retreat (1979–2001), which is opposite to the pattern for Antarctica as a whole. Although these regional variations have climatic, biological and biogeochemical consequences at the local scale, here we are interested in the annual cycle as a whole and in the fact that despite the substantial variation on wide-ranging time and space scales, the asymmetric annual cycle is consistent over the full measurement period.

6. How Well Do Climate Models Represent the Observed Antarctic Annual Cycle?

The CMIP is a standard protocol for studying the output of coupled atmosphere-ocean general circulation models established in 1995 by the Working Group on Coupled Modelling of the World Climate Research Programme. Phase 5 (CMIP5) is the most current and extensive of the CMIPs, but the planning for the sixth phase is well underway. Over 20 groups worldwide have contributed simulations to CMIP5 from their independently developed models, many of which include different physics and a range of complexity in sea ice components (Roach et al., 2018). Such coupled climate models run with realistic estimates of external climate forcings do not produce the slight increase in SIE that was discussed in section 3. Instead, they generally simulate a decreasing trend, but it is hard to identify how much of the discrepancy is due to inadequate representation of key processes in the models and how much is due to internal variability in SIE that the models do not capture (Shu et al., 2015).

As described in section 4.1.2, even though the observed trends cannot be fully explained by trends in the major climate modes, tropical forcing appears to drive a significant amount of the natural sea ice variability and ensuring that models simulate the changes in these modes is key to improving the representation of Antarctic sea ice. For example, (Meehl et al., 2016) showed that if models correctly simulate the timing of the observed negative IPO of the early 2000s, they are then able to simulate the midlatitude teleconnection pattern and associated increase in Antarctic sea ice. Note that by taking multimodel means, the internally generated decadal variability thought to be responsible for the observed trends in Antarctic sea ice (Gagné et al., 2015; Hobbs et al., 2015; Polvani & Smith, 2013; Turner et al., 2016) is averaged out (Meehl et al., 2014).

Arzel et al. (2006) assessed the ability of the CMIP3 climate models to capture the seasonal cycle in Antarctic sea ice and found that for the first 20 years of the satellite era, the multimodel mean SIE agreed reasonably well with that retrieved by satellite. Later, Turner et al. (2012) performed an assessment of the annual cycle and trends in Antarctic SIE for the 19 available models from the updated CMIP5. This analysis was repeated by Mahlstein et al. (2013), but they looked at SIA, which is the preferred metric in model evaluation studies (Notz, 2014). Zunz et al. (2013) and then Shu et al. (2015) each looked at SIE in 24 and 49 CMIP5 models, respectively, but did not discuss the seasonal cycle.

Representations of Antarctic sea ice in CMIP5 models did not improve significantly compared to CMIP3, but the seasonal cycle of observed SIE is reasonably well-represented by the multimodel ensemble mean, albeit with a large inter-model spread (Figure 7a). The majority of models do not have enough sea ice coverage at the minimum in February (i.e., they are melting too much of the ice in summer), while several models have less than two thirds of the observed SIE at the September maximum. Zunz et al. (2013) concluded that no CMIP5 model can reproduce a reasonable agreement with satellite observations and that all models overestimate the interannual variability of Antarctic SIE, particularly in winter. Roach et al. (2018) pointed out that these tendencies are broadly consistent across the CMIP5 simulations, despite the variety of complexity of sea ice physics incorporated in these models.

An analysis of the models used in the Turner et al. (2012) study shows that the maximum root mean square error in modeled SIE compared to satellites is $9.2 \times 10^6 \text{ km}^2$ (half of the maximum satellite ice extent and three quarters of the mean satellite SIE). The mean root mean square error is $3.8 \times 10^6 \text{ km}^2$ (just under a third of the mean satellite SIE). However, of the 19 models that were available at the time of their study, only

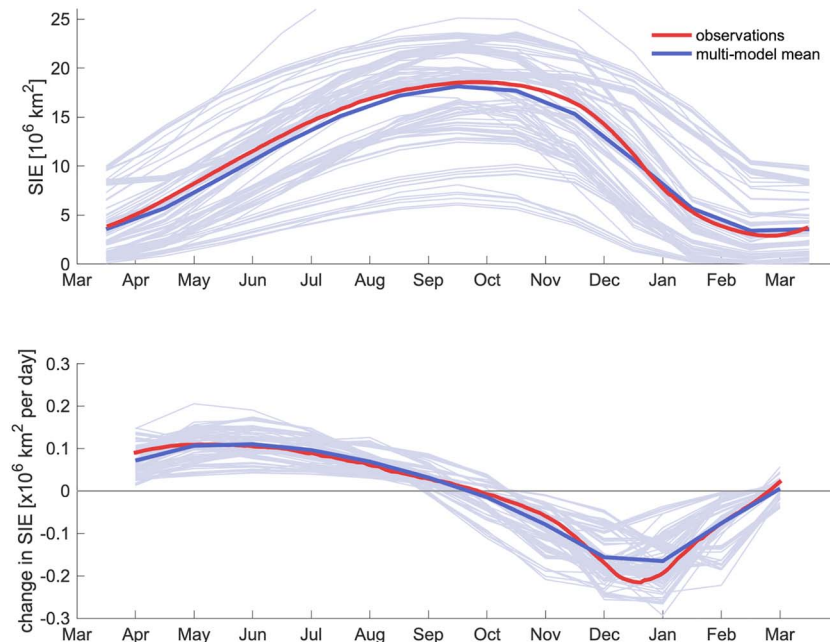


Figure 7. (a) Antarctic SIE from the CMIP5 models. The faint blue lines show the climatology of monthly sea ice extent (averaged over 1980–2010) for 118 simulations from 40 CMIP5 models, using the Historical (1850–2005) and RCP4.5 (2006–2100) experiments. We note that the choice of RCP scenario has minimal influence on the years 2006–2010 (Rosenblum & Eisenman, 2017). The thick blue line is the multimodel mean, with all 118 simulations equally weighted, and the red line is the observed mean (blue line) from Figure 5a. (b) Rate of change of Antarctic SIE from the CMIP5 models. The faint blue lines give the climatology for each individual simulation, where the daily rates were computed from monthly values, divided by number of days per month, to enable direct comparison with Figure 6. The thick blue line shows the multimodel mean, as in panel (a). The red line is the observed rate of change (blue line) from Figure 6b. SIE = sea ice extent; RCP = representative concentration pathway.

2 have a symmetric seasonal cycle. Of the remaining 17, 6 display a seasonal cycle that is too asymmetric (8 months growth vs. 4 months melt instead of 7 months growth vs. 5 months melt). Although there are major deficiencies in the magnitude of the seasonal cycle, the asymmetric pattern and its timing are largely captured by climate models, suggesting that on the whole, climate models already include the mechanisms that drive the asymmetric cycle of Antarctic sea ice.

Rosenblum and Eisenman (2017) processed the SIE in 118 simulations from 40 CMIP5 models (averaged over 1980–2010); climatological Antarctic SIE and its rate of change in these simulations are shown in Figure 7, and it is clear that none of these simulations have an ice growth season that is shorter than the melt season. For 22 simulations the growth and melt season are symmetric, lasting 6 months each. For 73 simulations the growth season lasts 7 months, for 23 simulation it lasts 8 months. In the multimodel mean, the growth season is 7 months, followed by 5 months of melt, very similar to the observations.

7. Main Mechanisms Controlling the Asymmetric Antarctic Annual Sea Ice Cycle

Two processes have been proposed as most likely to control the asymmetric pattern of Antarctic sea ice growth and melt: the SAO in the surface pressure, which modulates the position of the ice edge through the associated wind field and related Ekman forcing (Enomoto & Ohmura, 1990), and the ice-ocean albedo feedback, which is a major factor in seasonal sea ice retreat (Kashiwase et al., 2017).

Intra-annual variability in Antarctic sea ice concentration has been linked by several authors to the SAO of the circumpolar trough (Enomoto & Ohmura, 1990; Watkins & Simmonds, 1999). This mechanism is described more fully in the next section (7.1). The relationship between regions of divergence related to the position of the circumpolar trough relative to the sea ice edge is likely a key control for the rate of growth or retreat of the sea ice edge since the expansion or contraction of the sea ice edge is either working with or against Ekman transport. As will be discussed in section 7.1.1, the circumpolar trough is generally more

intense during spring than in autumn. Due to the SAO, this trough and the sea ice edge cross twice-yearly, once in autumn as the sea ice advances and again in spring as the ice retreats. In spring and summer, the easterlies aid in the rapid retreat of the sea ice edge and during autumn and winter the westerlies assist in its expansion.

These regions of dynamical divergence also trigger a thermodynamic effect, which varies depending on the prevailing temperature of the upper ocean. In winter, cold open water areas can lead to an increase in new ice production, and therefore greater SIE, whereas in spring/summer these now warm open water regions can accelerate the melting of ice. Due to the ice-ocean-albedo feedback, areas of open water created by the prevailing wind field during spring/summer provide the heat needed to melt such a large quantity of ice in just a few months. The rapid spring melt is thereby facilitated by warming of the ocean mixed layer through solar radiation input (Nihashi & Cavalieri, 2006; Ohshima & Nihashi, 2005). There is some discussion in the literature about the role of deep ocean convection in contributing to the annual cycle of Antarctic sea ice (Gordon, 1981), but this has since been discounted as a major component of the consistently asymmetric Antarctic sea ice cycle, as will be discussed later in section 7.2.1.

7.1. The Atmospheric Circumpolar Trough and the SAO

Antarctica is encircled by a low-pressure zonal belt commonly known as the atmospheric CPT, which has also been referred to in the literature as “Atmospheric Convergence Lines” Enomoto and Ohmura (1990); Yuan and Li (2008). It can be depicted as a continuous belt of minimum pressure surrounding Antarctica that marks a boundary between westerlies to the north and easterlies to the south. Note that this band of minimum pressure is a net effect made up from the collective tracks of many individual storms.

Many SH climate variables, including cyclone density, display much more zonal symmetry than their NH counterparts (Simmonds & K, 2000); the SH atmospheric circulation is not dominated by jet stream entrance and exit regions to the same extent as the NH (Trenberth, 1991). The most intense cyclonic systems occur in a ring around the continent, usually located 60–70°S. The CPT is formed by large numbers of cyclones that have either migrated from midlatitudes or developed within the Antarctic sea ice or coastal zone (Jones & Simmonds, 1993; Turner et al., 1998) and fluctuations in its strength and position are indicative of changes in a much larger system of cyclonic activity (Meehl, 1991). In a statistical analysis of SH extratropical cyclones, Jones and Simmonds (1993) found that although there is little seasonality in the distribution of cyclones in the Southern Ocean, there is considerable seasonality in their central pressure, leading to an identifiable low-pressure belt that varies in both intensity and latitude.

The CPT is characterized by a twice yearly intensification and poleward contraction, followed by a weakening and expansion. This phenomenon is called the SAO. The SAO is a highly variable feature of the annual cycle of pressure and meridional temperature gradient (van Loon & Jenne, 1972) that was early on described by Reuter (1936) and then again more in more detail by Schwerdtfeger, (1960, 1963). Van Loon (1967) first discovered and documented the mechanism that produces the SAO, which is described further in the next paragraph, and then Meehl (1991) reviewed further work on this twice-yearly phenomenon. At middle and high latitudes in the SH, the annual cycle of mean sea level pressure is dominated by a strong half-yearly pattern that explains more than 50% of the variability in the sea level pressure (Raphael & Holland, 2006; Xu et al., 1990). The SAO occurs through the depth of the troposphere (Meehl, 1991) and is associated with similar fluctuations of tropospheric temperature gradients, geopotential heights, sea level pressure and winds at middle and high latitudes in the SH (van Loon, 1967; van Loon & Jenne, 1972; van Loon & Rogers, 1984). Most of the research on the SAO has focused on the atmosphere, but this twice-yearly signal has also been seen found in ocean currents (Large & van Loon, 1989) and ocean wind stress of the extratropics (Trenberth et al., 1990).

Van Loon (1967) established that the SAO in the meridional temperature gradient occurs due to differential cooling and heating rates between the Antarctic continent and the midlatitude polar oceans. Although the annual temperature ranges are similar near 50°S and 65°S, autumn cooling over the oceans near 50°S is more rapid than warming in spring, while the reverse is true near 65°S (Meehl, 1991; van Loon, 1967). This derives from the differing annual evolution of tropospheric temperature over the Southern Ocean and the Antarctic continent: in the midlatitudes, ocean heat storage delays the summer temperature maximum and winter minimum; the Antarctic continent has no such well-defined winter minimum (called a “coreless winter”), and instead temperatures drop rapidly in autumn and then decrease more gradually into early spring before rising rapidly into summer. This leads to an intensification of the temperature gradient twice a year in the

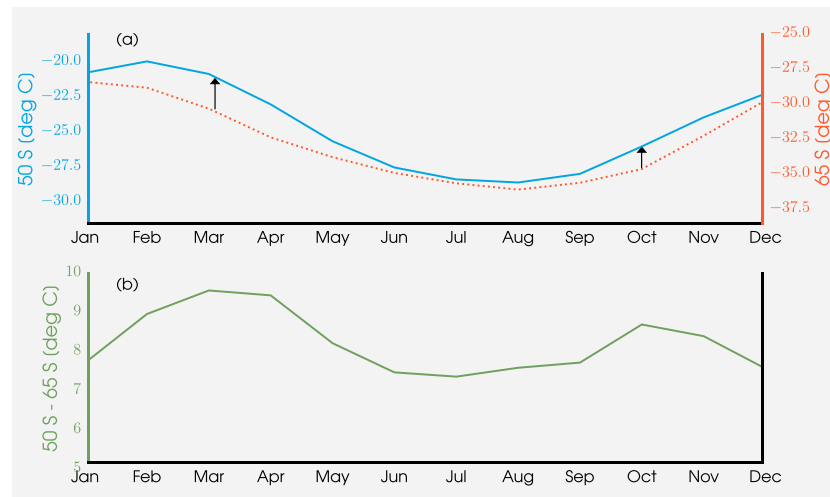


Figure 8. (a) Climatological cycle of European Centre for Medium-Range Weather Forecasts Re-Analysis-Interim monthly mean values of 500-hPa temperature at 50°S and 65°S (red), averaged over the years 1979–2016. Highlighted by the black arrows is the twice-yearly steepening of the meridional temperature gradient. (b) Temperature difference between monthly mean values at 50°S and 65°S.

midtroposphere (Figure 8). This increase of the temperature gradient (and therefore baroclinicity and storm activity) between the middle and high latitudes results in the strong half-yearly pattern in surface pressure.

Note that the SAO is different from the SAM, the dominant mode of circulation variability in the SH. Both SAM and SAO are zonally symmetric phenomena, but the SAM index is defined by the sea level pressure anomaly fields and is related to the strength of the midlatitude westerlies (Thompson & Solomon, 2002), while the SAO is defined in the mean sea level pressure fields and is a coupled ocean-atmosphere mode of variability (Walland & Simmonds, 1999). The SAO index is the zonal, mean sea level pressure between 50°S and 65°S (Meehl, 1991), whereas there are a number of ways to derive the SAM index, including two station-based indices (Marshall, 2003; Visbeck, 2009), the normalized zonal mean sea level pressure between 40°S and 65°S (Gong & Wang, 1999), the normalized zonal mean sea level pressure between 40°S and 70°S (Nan & Li, 2003), and the leading empirical orthogonal function of sea level pressure anomalies south of 20°S (Thompson & Wallace, 2000). These two climate modes share a large amount of variance; the main difference between them is that pressure variability over the Antarctic continent contributes substantially to the SAM variability but not necessarily to the SAO variability (Yuan & Li, 2008). Yuan and Li (2008) also showed that the SAM is dominated by decadal variability whereas the half-year cycle overwhelmingly dominates the SAO spectrum. Both of these indices are found in the dominant time scales of variability over the Southern Ocean (Cerrone et al., 2017). The SAM has further been shown to modulate SIE: positive values of the summertime SAM are followed by increased SIE during autumn and negative SAM during the 2016/2017 austral summer contributed to the record minimum SIE in March 2017 (Doddridge & Marshall, 2017). While the SAM is seen as a driver of the interannual variability of SIE, it is the SAO and its half-yearly cycle that is thought to play a key role in controlling the asymmetric growth-melt cycle in Antarctic sea ice. However, this role has yet to be quantified and remains a gap in our understanding at present.

7.1.1. SAO Index

Van Loon (1967) first developed an index for the SAO, computed from the 500 hPa temperature difference between 50°S and 65°S, using observational station data across the SH. Van Loon's index is linked to the idea that the twice-yearly intensification of the midtroposphere temperature gradient between the ocean-dominated middle latitudes and the polar continental latitudes is associated with a twice-yearly increase of storm activity and therefore changes in intensity of the CPT. However, another index, calculated from the difference in zonal, annual mean sea level pressure between 50°S and 65°S (Meehl et al., 1998; Raphael & Holland, 2006; Taschetto et al., 2007) to reflect the magnitude of the meridional gradient in sea level pressure between these two latitudes, is more appropriate for directly examining the influence on the CPT. 65°S best represents the temporal characteristic of the SAO since the half-yearly cycle in sea level pressure dominates in the Antarctic coastal region, while the annual cycle dominates on the Antarctic plateau (van den Broeke, 1998).

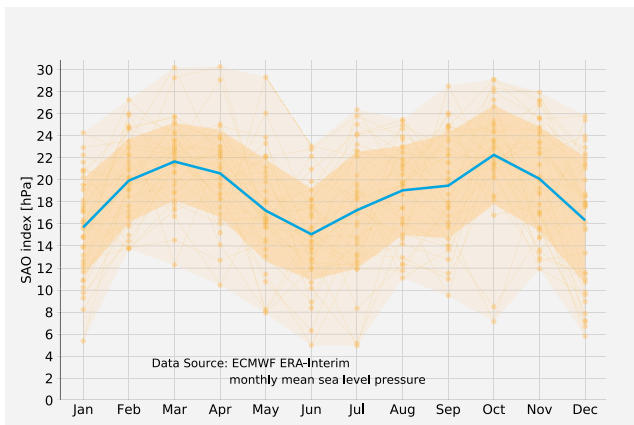


Figure 9. The blue line shows the SAO index: semi-annual cycle of change in the mean sea level pressure between 50°S and 65°S derived from ERA-Interim monthly mean sea level pressure (1979–2016). The yellow dots show the monthly SAO Index for all the years in the record. The dark yellow shading is one standard deviation away from the mean, and the pale yellow shading shows the full range of the data across all the years in the record. SAO = Semiannual Oscillation; ECMWF = European Centre for Medium-Range Weather Forecasts; ERA = ECMWF Re-Analysis.

There is greater variation in the timing and intensity of the March peak in the SAO compared to the October peak. As discussed earlier, this is due to the deepest cyclones passing through the region of the CPT during spring (Walland & Simmonds, 1999).

Figure 9 is based on data for 1979–2016. However, this annual pattern of tropospheric pressure changed appreciably after the late 1970s, when the atmospheric reanalysis data set begins. Historical station data from New Amsterdam Island in the Indian Ocean (38°S, 78°E), Chatham Island in the Pacific (44°S, 177°W) and Gough Island in the Atlantic (40°S, 10°W) provides evidence of a change in the SH middle and high latitudes that began just before 1980 (Hurrell & van Loon, 1994). They suggest that the SAO was stronger pre-1979, with the second peak in September as opposed to the post-1979 peak on October and attributed these changes to a concurrent rise of SSTs at lower latitudes. Post-1979, the tropospheric polar vortex, which pre-1979 weakened after a peak in late September, remained strong into November and the breakdown of the stratospheric polar vortex was similarly delayed. Note that this weakening of the SAO since the 1970s is concurrent with a poleward intensification of the westerlies that encircle Antarctica. Meehl et al. (1998) attributed the weakened SAO to changes in the temperature gradient between 50 and 65°S.

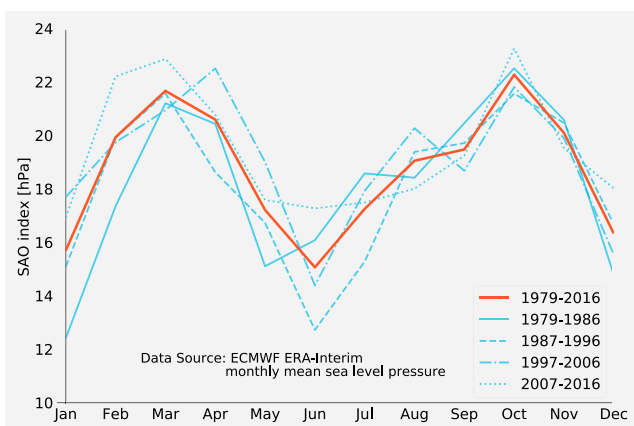


Figure 10. SAO index derived from ERA-Interim monthly mean sea level pressure, by decade. The thick red line shows the overall SAO index for 1979–2016; the thin blue lines show 10-yearly means. SAO = Semiannual Oscillation; ECMWF = European Centre for Medium-Range Weather Forecasts; ERA = ECMWF Re-Analysis.

Figure 9 shows the SAO index as defined in Meehl et al. (1998) and derived from the ECMWF ERA-Interim monthly surface pressure reanalyses for 1979–2016 (Dee et al., 2011). In the 1979–2016 average the strongest pressure difference is in October, which is slightly higher than in March. In general, the CPT is slightly deeper in spring than autumn since the deepest cyclones through the region of the CPT occur in spring (Jones & Simmonds, 1993; Walland & Simmonds, 1999). Although the mean SAO index for the full 38-year ERA-Interim record is shown here, the half-yearly pattern with peaks in intensity in spring and autumn and troughs in winter and summer is consistent throughout. A key part of the conceptual model first described by Enomoto and Ohmura (1990) is that the position of the CPT and the position of the ice edge cross twice-yearly every year (see section 7.1.3).

7.1.2. Variation in the SAO

There is considerable interannual variation in the SAO index (Figure 9). This can be attributed to the seasonal intensity and latitudinal movement of the band of minimum pressure, which emerges from the collective tracks of individual cyclones (Meehl, 1991). Due to the high interannual variability seen in Figure 9, the decadal means are plotted in Figure 10 to illustrate how the SAO has changed over the data record. Although there is significant variation in the magnitude of the SAO, the semi-annual pattern is consistent and the timing of the peaks and troughs only varies by up to a month over the last 40 years, with no notable long-term trend.

Changes in this half-yearly cycle have been related to various mechanisms, including a rise in low latitude SSTs (Hurrell & van Loon, 1994), a breakdown of the polar stratospheric vortex (Thompson & Solomon, 2002) and a modification in the temperature gradient between 50°S and 65°S (Meehl et al., 1998). Simmonds and Jones (1998) have also shown that in both the middle and high latitudes, the temporal variability of the SAO of pressure is statistically related to the variability of the high-latitude temperature gradient and that low-frequency variability in the SAO depends on the ocean-atmosphere coupling at middle and high latitudes. Furthermore, ocean heat storage and the annual cycle of SST at 50°S seem critical to the phase and the amplitude of the SAO, as argued by Meehl (1991) in a modeling study.

7.1.3. Influence of the CPT on the Sea Ice Edge

The variation in intensity and position of the CPT follows a half-yearly oscillation: the CPT contracts (moves south) and deepens in March and

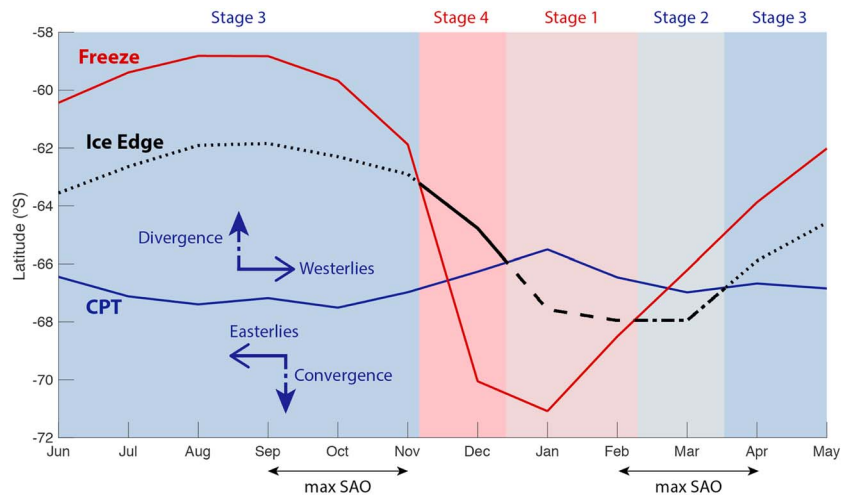


Figure 11. The thermal (freezing or melting) and dynamic (divergence or convergence) conditions in the marginal sea ice zone, following Enomoto and Ohmura (1990) but updated for the full data record (1979–2016). The black line shows the mean latitude of monthly Antarctic sea ice extent as calculated from the National Oceanic and Atmospheric Administration/National Snow and Ice Data Center Climate Data Record (Fetterer et al., 2017). The blue line shows the mean latitude of the circumpolar trough from ERA-Interim monthly mean sea level pressure: The SAO is strongest in regions identified by the horizontal black arrows. The red line shows the mean latitude of the freezing temperature ($-1.8\text{ }^{\circ}\text{C}$) from ERA-Interim monthly 2-m air temperature. Westerlies to the north (south) of the CPT lead to divergence (convergence). ERA = European Centre for Medium-Range Weather Forecasts Re-Analysis; SAO = Semiannual Oscillation; CPT = Circumpolar Trough.

September/October and expands (moves north) and weakens in June and December/January, as seen in the SAO index (Figure 9). This seasonal strengthening and poleward intensification helps to explain the mean asymmetric pattern of the timing of annual ice edge advance (slow, over 7 months between March and September) and retreat (fast, over 5 months between October and February) according to a conceptual model first described by Enomoto and Ohmura (1990).

A key component of this conceptual model is the fact that the low-pressure minimum defining the CPT marks a boundary between westerlies to the north and easterlies to the south. The westerly winds bestow a northward Ekman component on ice motion, whereas the easterly winds impart a southward component, so the CPT is a region of divergence. Depending on the location of the ice edge in relation to the CPT, this leads to either divergence or convergence of sea ice. The type of ice that is influenced by the CPT is also important: winds have a greater influence in the marginal ice zone compared to the pack ice due to the lower concentrations and the greater proportion of open areas and thinner ice.

Convergence usually results in increased sea ice concentration but lower SIE, whereas divergence can mean either smaller or larger SIE depending on the prevailing temperatures. In winter the open water fills with new ice and the ice field expands accordingly, spreading northward as a function of the total divergence within the existing ice field (Gordon & Taylor, 1975). After the spring equinox, open water regions within the ice field increase heat absorption by the ocean, and rapid ice melting follows. The half-yearly variation in the strength and location of the divergence and the related latitudinal variation between northward and southward transport in relation to the location of the ice edge are the drivers of asymmetric changes in ice extent in this conceptual model.

Figure 11 is based on Figure 14 from Enomoto and Ohmura (1990), but the data set is extended to the full available record (1979–2016), whereas the Enomoto and Ohmura (1990) figure is based on data from 1982–1984. The positions of the CPT, sea ice edge and atmospheric freezing isotherm are mean positions for each month for 1979–2016. The positions of the CPT and freezing temperature are derived from the ERA-Interim mean sea level pressure and 2-m air temperature, respectively. The freezing isotherm shown on Figure 11 is the $-1.8\text{ }^{\circ}\text{C}$ isotherm in the 2-m air temperature and is therefore an indication of the potential for freezing, rather than an absolute freezing line. Figure 11 indicates that from February to November, the ocean around Antarctica could freeze. It is interesting to note that although the thermal and dynamic conditions have large interannual variation, our Figure 11 is very similar to Figure 14 from Enomoto and

Ohmura (1990). This reinforces the fact that although all the components of the system have large temporal and spatial variability, when considered as a climatological mean, the pattern of the position of the sea ice edge relative to the location of the circumpolar trough remains remarkably consistent.

The mean monthly latitude of the sea ice edge is demarcated by the black line in Figure 11. When the sea ice edge (black line) coincides is south of the freezing line (the red line), then at this latitude and time of year the atmosphere is below -1.8° , the temperature at which sea water will start to freeze. When the sea ice edge (black line) is south of the CPT (blue line), the sea ice edge is subject to the easterlies located south of the circumpolar trough and the properties of the wind field tend to cause convergence in the marginal ice zone and the ice edge is driven toward the continent by Ekman forcing. On the other hand, when the ice edge is north of the CPT, the associated Ekman transport leads to divergence within the ice pack. The combinations of freezing versus melting conditions and convergence versus divergence produce four stages in this conceptual model (as shown in Figure 11).

At the beginning of the growing season in late February and March, the freezing line is northward of the sea ice edge, the ocean starts to freeze and the sea ice edge gradually begins to advance (Stage 2 in Figure 11). The CPT is furthest south and deepest during March (Figure 11 and Figure 9) and the expansion of the ice edge is therefore constrained by easterly winds and their associated southerly Ekman advection. The ice edge advances as the CPT starts to weaken until it eventually moves equatorward of the CPT location by late March (moving from Stage 2 to Stage 3). From the end of March onward, the ice edge expands northward with the Ekman transport associated with the westerly winds north of the CPT (Stage 3), but the intensity of the CPT is weak throughout this part of the growth period. As the ice edge moves further away from the CPT, the effect is further reduced and winter freezing conditions mean that the dynamic response becomes more sluggish as winter progresses. During this period, divergence within the marginal ice zone opens up regions of the pack, that now freeze due to the cold air temperatures. However, where ice concentration is high, the sea ice may have a tendency to converge along the CPT owing to an increase of the internal force (Hibler, 1986). At its maximum extent, the sea ice edge is considered to be in dynamic and thermal equilibrium.

As the maximum SIE approaches during August/September, the CPT again starts to move poleward and intensify, until it again reaches south of the ice edge (Stage 3 to Stage 4). Westerly winds north of the trough promote ice edge expansion due to northward Ekman forcing and easterly winds south of the trough support high sea ice concentrations near the coast due to southward Ekman forcing. This leads to a divergence of sea ice that creates areas of open water that now may not freeze due to warmer temperatures (Stage 4). Ice pushed north of the CPT during November is advected into warmed waters where it melts, which hastens the retreat of the ice edge. During spring and early summer, the CPT moves close to and eventually north of the ice edge and this contributes to a rapid retreat due to the southward Ekman forcing on the now low sea ice concentrations. The divergence of sea ice and the reduction of new ice formation work together to reduce the mean sea ice concentration.

This conceptual model was first described by Enomoto and Ohmura (1990) and wind-driven Ekman forcing of sea ice that it builds on is well-documented in the literature. As early as 1986, Hibler (1986) showed that the dynamic movement of sea ice in spring is an important factor in the rapid decay of the spring sea ice cover. Cavalieri and Parkinson (1981) demonstrated a relationship between the longitudinal distributions of the synoptic atmospheric circulation and the distribution of regional SIE. The relative location of the CPT with the ice edge was also shown by both Watkins and Simmonds (1999) and Stammerjohn et al. (2003) to influence the timing of sea ice advance and retreat via wind-driven sea ice drift in the Western Antarctic Peninsula.

This mechanism is also supported by Stroeve et al. (2016) who assessed the variability of the marginal ice zone, ice pack and coastal polynyas between the NASA Team and Bootstrap algorithms. They showed that an initial peak in the marginal ice zone coverage coincides with the maximum extent of consolidated ice pack, but that unlike the consolidated ice, which starts to retreat by the end of September, the percentage of marginal ice stays nearly constant at this maximum extent until the end of November. This is consistent with the description above whereby the pack ice first undergoes divergence due to the CPT being located south of the ice edge. At both a local and an Antarctic-wide scale, the interplay between the location of the sea ice edge and the dynamical influence of the mean wind field has been shown to be an important influence on the advance and retreat of the sea ice edge.

7.2. Sources of Heat for Rapid Melting: Ice-Ocean-Albedo Feedback Versus Ocean Convection

The section above provides a description of the dynamical processes that drive the asymmetric pattern in sea ice formation and melt. However, a large amount of energy is required to melt the ice in just a few months and the heat flux required to melt such a large quantity of ice in just a few months is the other part of the picture needed to provide a complete description of the asymmetric pattern in the seasonal cycle. Gordon (1981) suggested that the atmosphere-to-ocean heat flux is insufficient to account for the massive ice melt between mid-November and mid-January and that open water regions induced by Ekman divergence must play a role.

Sea ice ablation processes are distinctly different in the Arctic and the Antarctic. Calculated net heat flux suggests that surface melting of the sea ice cover and the subsequent formation of meltponds is small in the Antarctic, unlike that for the Arctic (Andreas & Ackley, 1982). Drinkwater and Liu (2000) have argued from satellite data sets that areas of surface melting are sparse and short-lived in the Antarctic sea ice zone and that atmospherically induced surface melting and resulting albedo feedback is not the dominant mechanism responsible for melting. They show that absorption of summer shortwave radiation by open regions in the ice that dominates the melting process. Indeed, the processes of ice melting on the bottom and lateral faces due to heat input through open water areas has been long known to be important in Antarctica. Parkinson and Washington (1979) first incorporated bottom and lateral melting in their large-scale ice-ocean coupled model and could roughly reproduce the seasonal cycle of sea ice, even when excluding dynamical processes. There is a large fraction of open water due to divergent drift in the Antarctic (Drinkwater & Liu, 2000; Jeffries et al., 1994) and these regions of open water can be warmed either by the atmosphere (in the absence of ice) or from warm water upwelling. The relative importance of these two mechanisms on the fast retreat of Antarctic sea ice has been extensively discussed in the literature. We summarize some of this work and argue that the ice-ocean-albedo feedback plays a significant role in the rapid spring melt.

7.2.1. Ocean Convection

One potential source of heat for the rapid melt of sea ice in spring is the upward mixing of ocean heat due to the divergence imparted by westerlies to the north of the CPT and easterlies to the south. The Southern Ocean is only marginally stable (Martinson, 1990) and the Antarctic sea ice zone is characterized by the presence of CDW below the mixed layer. CDW is warm compared to the surface water so any decrease in the stability of the water column could lead to warmer surface ocean temperatures that can also melt sea ice.

Early thinking was that upward mixing of ocean heat due to Ekman upwelling caused by the divergence and cross-pycnocline mixing processes could accelerate the melting of thin ice and enhance sea ice retreat (Gordon, 1981). Since then, the contribution of upward mixing of ocean heat to the rapid spring melt has been argued to be small by various authors due to the fact that melting ice freshens and stabilizes the water column (Figure 4). The mixed layer depth (MLD) under sea ice has a marked seasonality. In winter there is a large MLD associated with convection when sea ice forms and releases brine. The downward transport of salt released in winter increases the MLD, weakens the stability and leads to potential overturning of the water column. During winter there is therefore an opportunity for deep water convection to play a role in retarding the growth of sea ice, however stability is generally maintained during winter by oceanic diffusive and entrainment heat fluxes (Martinson, 1990). Due to a strong thermal gradient across the pycnocline, there is a strong diffusive heat flux of 26 W/m^2 , according to Martinson (1990) and this prevents significant ice growth, which would otherwise destabilize the water column through brine rejection. This is further supported by modeling experiments conducted by Wilson et al. (2019), who showed that the heat entrained into the mixed layer is able to suppress ice growth and limit further erosion of the pycnocline. As the season progresses the rate of ice growth decreases, reflecting the increase in net oceanic heat flux.

During spring there is a small MLD when sea ice melts and freshwater stabilizes the upper ocean column (Figure 4). Therefore, entrainment from the deeper ocean is suppressed in the spring due to this strong stratification of the ocean surface layer by both heating and melting. The freshwater due to melting is incorporated into a shallow mixed layer. Based on a heat budget analysis, Nihashi and Ohshima (2001) showed that an assumed spatially uniform flux of 10 W/m^2 from the deeper ocean is less than a quarter of the total heat input through open water from the atmosphere during the active melt period (December–January), making the heat flux over open water the most significant contribution to the spring melt. This is further supported by a follow-up study (Ohshima & Nihashi, 2005) that neglected deep ocean heat flux in their simple bulk ice-upper ocean coupled model but could still reproduce the fast melt of Antarctic sea ice.

It is thus generally accepted that deep ocean convection does not play a significant role in melting sea ice in the annual seasonal cycle, but that it does play a small role in slowing the ice growth through the winter. Instead, in the summer Antarctic sea ice zone, heat input into the ice-upper ocean system mainly occurs over the open water areas and this heat input is the main heat source for sea ice decay as discussed in the next section.

7.2.2. Ice-Ocean-Albedo Feedback

The ice-ocean-albedo feedback, also referred to as “open water-albedo feedback” (Ackley et al., 2001), is an important feedback process during sea ice decay. This is different from the ice-albedo feedback whereby decreasing surface albedo due to surface melt causes an increase in solar radiation absorption (Curry et al., 1995). Instead of being a modification in the surface albedo of snow/ice, the ice-ocean-albedo feedback is an areal albedo change due to a varying open water fraction (Nihashi & Cavalieri, 2006). Most of the Antarctic sea ice zone is seasonal and much of the ice surface is covered by snow with a high albedo. Open water has a much lower albedo than sea ice, and therefore can absorb a large amount of solar radiation in summer (Maykut & McPhee, 1995) and this heat can become the dominant heat source for bottom and lateral melting of sea ice (Maykut & Perovich, 1987). In the absence of clouds, the albedo of open water is typically 0.06, while bare sea ice depends on temperature, age and state of the surface (Maykut, 1986) and varies from approximately 0.5 to 0.7. Snow has an even higher albedo and snow-covered ice can reflect as much as 90% of the incoming solar radiation.

In the ice-ocean-albedo feedback, as the ice concentration decreases in spring, heat input to the upper ocean is enhanced due to larger absorption of solar radiation in the increased open water area, leading to a further decrease in ice concentration through the sea ice melt by the oceanic heat (Nihashi & Cavalieri, 2006). The open water area is enhanced through the feedback mechanism and leads to increased absorption of solar energy in the upper ocean. In a modeling study, Hunke and Ackley (2001) showed that the open water area within the Ronne polynya was enhanced by melting through this feedback mechanism.

In a heat budget analysis based on ECMWF atmospheric reanalysis and in situ data, Nihashi and Ohshima (2001) demonstrated that net heat input at the water surface from the atmosphere during the time of maximum melt (December) reaches 100–150 W/m² as a result of solar heating. This is one or two orders of magnitude larger than the heat input at the ice surface (less than 10 W/m²) because of the albedo difference. Most of the sea ice surface in the Antarctic Ocean is covered by snow, which has a higher albedo than ice. Furthermore, Nihashi and Ohshima (2001) showed that the total heat input into the upper ocean through areas of open water is comparable to the latent heat of sea ice decay for the entire Antarctic sea ice zone.

Fichefet and Maqueda (1997) demonstrated in a modeling study that sea ice decay is considerably suppressed when solar radiation input in the upper ocean is removed. When they maintained ice concentration at 100% to simulate the effect of regions of open water on the seasonal cycle of sea ice, they found that the retreat of the SH ice cover in spring was markedly reduced. This suggests that the heat supplied to the upper ocean from the atmosphere and subsequent lateral and bottom melting of sea ice are the main factors in Antarctic sea ice decay. In their heat budget analysis, Nihashi and Ohshima (2001) showed that heat through the open water area from the atmosphere is comparable to the latent heat of sea ice melting in the whole Antarctic sea ice zone and much larger than the estimated heat from the deeper ocean. The importance of the ice-ocean-albedo feedback was further supported in modeling studies by Ogura (2004) and Ohshima and Nihashi (2005), who also found that including divergent wind effects improved their results.

8. Summary

Antarctic sea ice has shown a modest increasing trend over the last four decades, albeit with record low SIE. The overall increasing trend is made up of substantial regional changes, with increases in the Ross Sea and a decrease in the Amundsen and Bellingshausen seas. It is clear that different drivers are dominant for different regions and seasons, but surface winds play a key role. One of the major difficulties is that observations are sparse and the variability is strong. Climate models do not capture key features of Antarctic sea ice cover and, for now, remain limited tools to examine the importance of different drivers of sea ice change.

The asymmetric cycle in Antarctic sea ice is an interesting phenomenon because it occurs so regularly on a background of large interannual variability. The annual growth and melt of Antarctic sea ice is the largest seasonal ice growth and melt cycle on the planet. Sea ice plays a key role in mediating exchange between the

atmosphere and ocean, and is an important habitat for the diverse and unique Southern Ocean ecosystem. Therefore, understanding and being able to model this phenomenon is of broad interest.

There have been a number of studies looking at the effect of winds and the ice-ocean-albedo feedback on long-term changes to the sea ice cover in both the Arctic and the Antarctic. It is clear that these processes work together on an annual basis to create the very regular shape of the seasonal SIE climatology. The SIE in the Antarctic is extremely variable from year to year, but yet it retains the asymmetric characteristic pattern of slow growth and fast melt. The CPT changes in terms of intensity and location but is always characterized by the SAO. Despite the large variations of both the sea ice edge and the CPT on a range of time and space scales, the ice edge always crosses the CPT twice each year in March/April and December. The associated winds either assist or work against sea ice growth and retreat; open water regions created by divergence in the spring then facilitate rapid melting through the ice-ocean albedo feedback. In addition to lateral and bottom melting of the ice, the increased melting due to this feedback mechanism breaks up the floes. This adds to the feedback process since smaller floes melt much more quickly.

This overall pattern masks regional differences which are likely to be of major importance for local ecosystems. In order to understand sea ice variability across different regions, the varying influences of contributing processes such as surface winds, the dynamic and thermodynamic processes in the ice pack, the interaction with the Southern Ocean, the modification of the hydrological cycle, and interaction with atmospheric indices such as ENSO and SAM need to be considered. It is clear that total SIE is ill suited for regional studies looking at the influence of sea ice variability (Raphael & Hobbs, 2014). However, the regularity of the asymmetric seasonal cycle in Antarctic sea ice is a striking phenomenon and this review brings together a description of likely mechanisms that maintain this remarkably consistent pattern of advance and retreat.

Glossary

Antarctic circumpolar trough (CPT) Band of low pressure that surrounds the Antarctic continent that is created due to the net effect of many individual storms. Also referred to as Atmospheric Convergence Lines (ACL) in the literature.

Coupled Model Intercomparison Project (CMIP) The CMIP provides a very useful platform for studying climate change by providing a community-based infrastructure in support of climate model diagnosis, validation, intercomparison, documentation, and data access. Simulations and projections by more than 60 state-of-the-art climate models and Earth system models are archived under CMIP5, the fifth and most recent, available data set.

Ice-Albedo feedback Decreasing surface albedo due to surface melt causes an increase in solar radiation absorption.

Ice-Ocean-Albedo feedback As the ice concentration decreases in spring, heat input to the upper ocean is enhanced due to larger absorption of solar radiation in the increased open water area, leading to a further decrease in ice concentration through the sea ice melt by the oceanic heat.

Representative concentration pathways (RCPs) A representative concentration pathway is a greenhouse gas concentration (not emissions) trajectory adopted by the IPCC for its fifth Assessment Report (AR5) in 2014. Four pathways have been selected for climate modeling and research, which describe different climate futures, all of which are considered possible depending on how much greenhouse gases are emitted in the years to come. The RCPs are consistent with a wide range of possible changes in future anthropogenic (i.e., human) greenhouse gas emissions, and aim to represent their atmospheric concentrations.

Sea ice area (SIA) The total area of ice coverage for a given domain—this is subtly different to SIE as it takes into account regions of open water within the ice pack. SIE is more commonly cited as there are fewer uncertainties associated with the satellite record, but SIA is the more robust metric for assessing models.

Sea ice concentration (SIC) A pixel/grid-scale observation defined as the fraction of ocean area that is covered by sea ice.

Sea ice duration Represents the period in days per year that a location (pixel/grid square) is covered by sea ice.

Sea ice extent (SIE) The total area of sea ice coverage with a sea ice concentration greater than some threshold value (typically 15%, which is used here). Sea ice change and variability are often described in

terms of SIE and it can be calculated over a range of domains: total circumpolar region, specific sectors or as a continuous function of longitude.

Sea ice intensification The rate of change of sea ice concentration.

Semiannual Oscillation (SAO) The twice-yearly intensification and poleward contraction of the Antarctic circumpolar trough.

Southern Annual Mode (SAM) A measure of the middle-to-high-latitude atmospheric pressure gradient that reflects the strength and position of the westerly winds that circle Antarctica.

Acronyms

CDR	Climate Data Record
CMIP3	Coupled Model Intercomparison Project Phase 3
CMIP5	Coupled Model Intercomparison Project Phase 5
CPT	Antarctic Circumpolar Trough
ECMWF	European Centre for Medium-Range Weather Forecasts
ENSO	El Niño Southern Oscillation
IPO	Inter-decadal Pacific Oscillation
RCPs	Representative Concentration Pathways
SAM	Southern Annular Mode
SAO	Semiannual oscillation
SIE	Sea Ice Extent

Acknowledgments

This work was funded by NYUAD Center for global Sea Level Change project G1204. Sea ice data were obtained from NSIDC Sea Ice Index (<https://nsidc.org/data/G02135>) and Climate Data Record (<https://nsidc.org/data/G02202>). ERA-Interim monthly reanalysis data sets were obtained from the ECMWF data archive (<https://www.ecmwf.int/en/forecasts/datasets/archive-datasets/reanalysis-datasets/era-interim>). We acknowledge Ian Eisenman for the processed CMIP5 data used in this study, available at <http://eisenman.ucsd.edu/code.html>. We would like to thank Philip Rodenbough and the Scientific Writing Program at New York University Abu Dhabi.

References

- Abram, N. J., Wolff, E. W., & Curran, M. A. J. (2013). A review of sea ice proxy information from polar ice cores. *Quaternary Science Reviews*, 79, 168–183. Retrieved from <https://doi.org/10.1016/j.quascirev.2013.01.011>
- Ackley, S. F., Geiger, C. A., King, J. C., Hunke, E. C., & Comiso, J. C. (2001). The Ronne polynya of 1997–1998: Observations of air-ice-ocean interaction. *Annals of Glaciology*, 33(1), 425–429.
- Ackley, S., Wadhams, P., Comiso, J. C., & Worby, A. P. (2003). Decadal decrease of Antarctic sea ice extent inferred from whaling records revisited on the basis of historical and modern sea ice records. *Polar Research*, 22(1), 19–25.
- Andreas, E. L., & Ackley, S. F. (1982). On the differences in ablation seasons of Arctic and Antarctic sea ice. *Journal of the Atmospheric Sciences*, 39(2), 440–447.
- Arzel, O., Fichefet, T., & Goosse, H. (2006). Sea ice evolution over the 20th and 21st centuries as simulated by current AOGCMs. *Ocean Modelling*, 12(3–4), 401–415.
- Baines, P. G., & Fraedrich, K. (1989). Topographic effects on the mean tropospheric flow patterns around Antarctica. *Journal of the Atmospheric Sciences*, 46(22), 3401–3415.
- Bintanja, R., van Oldenborgh, G. J., Drijfhout, S. S., Wouters, B., & Katsman, C. A. (2013). Important role for ocean warming and increased ice-shelf melt in Antarctic sea-ice expansion. *Nature Geoscience*, 6(5), 376–379. <https://doi.org/10.1038/ngeo1767>
- Bracegirdle, T. J., & Marshall, G. J. (2012). The reliability of Antarctic tropospheric pressure and temperature in the latest global reanalyses. *Journal of Climate*, 25(20), 7138–7146.
- Bromwich, D. H., Nicolas, J. P., & Monaghan, A. J. (2011). An assessment of precipitation changes over Antarctica and the Southern Ocean since 1989 in contemporary global reanalyses. *Journal of Climate*, 24(16), 4189–4209. <https://doi.org/10.1175/2011JCLI4074.1>
- Bronslaer, B., Winton, M., Griffies, S. M., Hurlin, W. J., Rodgers, K. B., Sergienko, O. V., et al. (2018). Change in future climate due to Antarctic meltwater. *Nature*, 564(7734), 53–58.
- Cavalieri, D. J., & Parkinson, C. L. (1981). Large-scale variations in observed Antarctic sea ice extent and associated atmospheric circulation. *Monthly Weather Review*, 109(11), 2323–2336.
- Cerrone, D., Fusco, G., Simmonds, I., Aulicino, G., & Budillon, G. (2017). Dominant covarying climate signals in the Southern Ocean and Antarctic sea ice influence during the last three decades. *Journal of Climate*, 30(8), 3055–3072. <https://doi.org/10.1175/JCLI-D-16-0439.1>
- Ciasto, L. M., Simpkins, G. R., & England, M. H. (2015). Teleconnections between tropical Pacific SST anomalies and extratropical Southern Hemisphere climate. *Journal of Climate*, 28(1), 56–65.
- Clem, K. R., & Fogt, R. L. (2015). South Pacific circulation changes and their connection to the tropics and regional Antarctic warming in austral spring, 1979–2012. *Journal of Geophysical Research: Atmospheres*, 120, 2773–2792. <https://doi.org/10.1002/2014JD022940>
- Collins, M., Knutti, R., Arblaster, J., Dufresne, J.-L., Fichefet, T., Friedlingstein, P., et al. (2013). Long-term climate change: Projections, commitments and irreversibility. In T. F. Stocker, D. Qin, G.-K. Plattner, M. Tignor, S. K. Allen, J. Boschung, A. Nauels, Y. Xia, Bex, V., & P. M. Midgley (Eds.), *Climate change 2013: The physical science basis. Contribution of Working Group I to the Fifth Assessment Report of the Intergovernmental Panel on Climate Change* (pp. 1029–1136). Cambridge, United Kingdom and New York, NY, USA: Cambridge University Press. Retrieved from <https://doi.org/10.1017/CBO9781107415324.024>
- Comiso, J. C., Gersten, R. A., Stock, L. V., Turner, J., Perez, G. J., & Cho, K. (2017). Positive trend in the Antarctic sea ice cover and associated changes in surface temperature. *Journal of Climate*, 30(6), 2251–2267. <https://doi.org/10.1175/JCLI-D-16-0408.1>
- Comiso, J. C., & Nishio, F. (2008). Trends in the sea ice cover using enhanced and compatible AMSR-E, SSM/I, and SMMR data. *Journal of Geophysical Research*, 113, C02S07. <https://doi.org/10.1029/2007JC004257>
- Comiso, J. C., & Steffen, K. (2001). Studies of Antarctic sea ice concentrations from satellite data and their applications. *Journal of Geophysical Research*, 106(C12), 31,361–31,385.
- Curry, J. A., Schramm, J. L., & Ebert, E. E. (1995). Sea ice-albedo climate feedback mechanism. *Journal of Climate*, 8(2), 240–247.

- de Santis, A., Maier, E., Gomez, R., & Gonzalez, I. (2017). Antarctica, 19792016 sea ice extent: Total versus regional trends, anomalies, and correlation with climatological variables. *International Journal of Remote Sensing*, 38(24), 7566–7584. <https://doi.org/10.1080/01431161.2017.1363440>
- de Vernal, A., Gersonde, R., Goosse, H., Seidenkrantz, M. S., & Wolff, E. W. (2013). Sea ice in the paleoclimate system: The challenge of reconstructing sea ice from proxies—An introduction. *Quaternary Science Reviews*, 79, 1–8. <https://doi.org/10.1016/j.quascirev.2013.08.009>
- de la Mare, W. K. (2009). Changes in Antarctic sea-ice extent from direct historical observations and whaling records. *Climatic Change*, 92(3), 461–493. Retrieved from <https://doi.org/10.1007/s10584-008-9473-2>
- Dee, D. P., Uppala, S. M., Simmons, A. J., Berrisford, P., Poli, P., Kobayashi, S., et al. (2011). The ERA-Interim reanalysis: Configuration and performance of the data assimilation system. *Quarterly Journal of the Royal Meteorological Society*, 137(656), 553–597. <https://doi.org/10.1002/qj.828>
- Ding, Q., & Steig, E. J. (2013). Temperature change on the Antarctic Peninsula linked to the tropical Pacific. *Journal of Climate*, 26(19), 7570–7585.
- Ding, Q., Steig, E. J., Battisti, D. S., & Küttel, M. (2011). Winter warming in West Antarctica caused by central tropical Pacific warming. *Nature Geoscience*, 4(6), 398–403.
- Doddridge, E. W., & Marshall, J. (2017). Modulation of the seasonal cycle of Antarctic sea ice extent related to the Southern Annular Mode. *Geophysical Research Letters*, 44, 9761–9768. <https://doi.org/10.1002/2017GL074319>
- Drinkwater, M. R., & Liu, X. (2000). Seasonal to interannual variability in Antarctic sea ice surface melt. *IEEE Transactions on Geoscience and Remote Sensing*, 38(4), 1827–1842.
- Edinburgh, T., & Day, J. J. (2016). Estimating the extent of Antarctic summer sea ice during the Heroic Age of Antarctic exploration. *Cryosphere*, 10(6), 2721–2730. <https://doi.org/10.5194/tc-10-2721-2016>
- Eisenman, I. (2010). Geographic muting of changes in the Arctic sea ice cover. *Geophysical Research Letters*, 37, L16501. <https://doi.org/10.1029/2010GL043741>
- Enomoto, H., & Ohmura, A. (1990). The influences of atmospheric half-yearly cycle on the sea ice extent in the Antarctic. *Journal of Geophysical Research*, 95(C6), 9497–9511. <https://doi.org/10.1029/JC095iC06p09497>
- Ferreira, D., Marshall, J., Bitz, C. M., Solomon, S., & Plumb, A. (2015). Antarctic Ocean and sea ice response to ozone depletion: A two-time-scale problem. *Journal of Climate*, 28(3), 1206–1226.
- Fetterer, F., Knowles, K., Meier, W., Savoie, M., & Windnagel, A. K. (2017). Sea ice index, version 3 [Antarctica]. NSIDC: National Snow and Ice Data Center, Boulder, CO. <https://doi.org/10.7265/N5K072F8>. [Date accessed: 9 November 2017].
- Fetterer, F., Savoie, M., Mallory, S., Duerr, R., & Stroeve, J. (2017). NOAA/NSIDC Climate Data Record of passive microwave sea ice concentration, version 3 [Antarctica]. NSIDC: National Snow and Ice Data Center, Boulder, CO. <https://doi.org/10.7265/N59P2ZTG>. [Date accessed: 16 January 2018].
- Fichefet, T., & Maqueda, M. A. M. (1997). Sensitivity of a global sea ice model to the treatment of ice thermodynamics and dynamics. *Journal of Geophysical Research*, 102(C6), 12,609–12,646.
- Fogt, R. L., & Bromwich, D. H. (2006). Decadal variability of the ENSO teleconnection to the high-latitude South Pacific governed by coupling with the Southern Annular Mode. *Journal of Climate*, 19(6), 979–997.
- Fogt, R. L., Bromwich, D. H., & Hines, K. M. (2011). Understanding the SAM influence on the South Pacific ENSO teleconnection. *Climate Dynamics*, 36(7–8), 1555–1576.
- Fogwill, C. J., Phipps, S. J., Turney, C. S. M., & Golledge, N. R. (2015). Sensitivity of the Southern Ocean to enhanced regional Antarctic ice sheet meltwater input. *Earth's Future*, 3(10), 317–329.
- Gagné, M.-É., Gillett, N. P., & Fyfe, J. C. (2015). Observed and simulated changes in Antarctic sea ice extent over the past 50 years. *Geophysical Research Letters*, 42, 90–95. <https://doi.org/10.1002/2014GL062231>
- Gloersen, P. (1995). Modulation of hemispheric sea-ice cover by ENSO events. *Nature*, 373(6514), 503–506.
- Gloersen, P., Campbell, W. J., Cavalieri, D. J., Comiso, J. C., Parkinson, C. L., & Zwally, H. J. (1992). Arctic and Antarctic sea ice, 1978–1987. *Satellite Passive-Microwave Observations and Analysis*, 290, 149–154.
- Gong, D., & Wang, S. (1999). Definition of Antarctic oscillation index. *Geophysical research letters*, 26(4), 459–462.
- Goosse, H., Lefebvre, W., de Montety, A., Crespin, E., & Orsi, A. H. (2009). Consistent past half-century trends in the atmosphere, the sea ice and the ocean at high southern latitudes. *Climate Dynamics*, 33(7–8), 999–1016. <https://doi.org/10.1007/s00382-008-0500-9>
- Goosse, H., & Zunz, V. (2014). Decadal trends in the Antarctic sea ice extent ultimately controlled by ice-ocean feedback. *Cryosphere*, 8(2), 453–470. Retrieved from <https://doi.org/10.5194/tc-8-453-2014>
- Gordon, A. L. (1981). Seasonality of Southern Ocean sea ice. *Journal of Geophysical Research*, 86, 4193–4197. <https://doi.org/10.1029/JC086iC05p04193>
- Gordon, A. L., & Taylor, H. W. (1975). Seasonal change of Antarctic sea ice cover. *Science*, 187, 346–347.
- Hibler, W. D. (1986). Ice dynamics, *The geophysics of sea ice* (pp. 577–640). Boston, MA: Springer.
- Hobbs, W. R., Bindoff, N. L., & Raphael, M. N. (2015). New perspectives on observed and simulated Antarctic sea ice extent trends using optimal fingerprinting techniques. *Journal of Climate*, 28(4), 1543–1560. <https://doi.org/10.1175/JCLI-D-14-00367.1>
- Hobbs, W. R., Massom, R., Stammerjohn, S., Reid, P. P., Williams, G. D., & Meier, W. (2016). A review of recent changes in Southern Ocean sea ice, their drivers and forcings. *Global and Planetary Change*, 143, 228–250. <https://doi.org/10.1016/j.gloplacha.2016.06.008>
- Holland, P. (2014). The seasonality of Antarctic sea ice trends. *Geophysical Research Letters*, 41, 4230–4237. Retrieved from <https://doi.org/10.1002/2014GL060172>. Received.
- Holland, P., & Kwok, R. (2012). Wind-driven trends in Antarctic sea-ice drift. *Nature Geoscience*, 5(12), 872–875. <https://doi.org/10.1038/ngeo1627>
- Holland, M. M., Landrum, L., Kostov, Y., & Marshall, J. (2017). Sensitivity of Antarctic sea ice to the Southern Annular Mode in coupled climate models. *Climate Dynamics*, 49(5–6), 1813–1831.
- Holland, M. M., Landrum, L., Raphael, M., & Stammerjohn, S. (2017). Springtime winds drive Ross Sea ice variability and change in the following autumn. *Nature Communications*, 8(1), 731. Retrieved from <https://doi.org/10.1038/s41467-017-00820-0>
- Hosking, J. S., Orr, A., Marshall, G. J., Turner, J., & Phillips, T. (2013). The influence of the Amundsen–Bellingshausen Seas low on the climate of West Antarctica and its representation in coupled climate model simulations. *Journal of Climate*, 26(17), 6633–6648.
- Housego-Stokes, R. E., & McGregor, G. R. (2000). Spatial and temporal patterns linking southern low and high latitudes during South Pacific warm and cold events. *International Journal of Climatology: A Journal of the Royal Meteorological Society*, 20(7), 793–801.
- Hunke, E. C., & Ackley, S. F. (2001). A numerical investigation of the 1997–1998 Ronne polynya. *Journal of Geophysical Research*, 106(C10), 22,373–22,382.
- Hurrell, J. W., & van Loon, H. (1994). A modulation of the atmospheric annual cycle in the Southern Hemisphere. *Tellus A*, 46(3), 325–338.

- Ivanova, D. P., Gleckler, P. J., Taylor, K. E., Durack, P. J., & Marvel, K. D. (2016). Moving beyond the total sea ice extent in gauging model biases. *Journal of Climate*, *29*(24), 8965–8987.
- Ivanova, N., Pedersen, L. T., Tonboe, R. T., Kern, S., Heygster, G., Lavernge, T., et al. (2015). Inter-comparison and evaluation of sea ice algorithms: Towards further identification of challenges and optimal approach using passive microwave observations. *Cryosphere*, *9*(5), 1797–1817. <https://doi.org/10.5194/tc-9-1797-2015>
- Jacobs, S. S., & Comiso, J. C. (1997). Climate variability in the Amundsen and Bellingshausen Seas. *Journal of Climate*, *10*(4), 697–709.
- Jeffries, M. O., Shaw, R. A., Morris, K., Veazey, A. L., & Krouse, H. R. (1994). Crystal structure, stable isotopes ($\delta^{18}O$) and development of sea ice in the Ross, Amundsen and Bellingshausen Seas, Antarctica. *Journal of Geophysical Research*, *99*, 985–995.
- Jin, D., & Kirtman, B. P. (2009). Why the Southern Hemisphere ENSO responses lead ENSO. *Journal of Geophysical Research*, *114*, D23101. <https://doi.org/10.1029/2009JD012657>
- Jones, J. M., Gille, S. T., Goosse, H., Abram, N. J., Canziani, P. O., Charman, D. J., et al. (2016). Assessing recent trends in high-latitude Southern Hemisphere surface climate. *Nature Climate Change*, *6*(10), 917–926. Retrieved from <https://doi.org/10.1038/nclimate3103>
- Jones, D. A., & Simmonds, I. (1993). A climatology of Southern-Hemisphere extratropical cyclones. *Climate Dynamics*, *9*(3), 131–145.
- Jones, R. W., Renfrew, I. A., Orr, A., Webber, B. G. M., Holland, D. M., & Lazzara, M. A. (2016). Evaluation of four global reanalysis products using in situ observations in the Amundsen Sea Embayment, Antarctica. *Journal of Geophysical Research: Atmospheres*, *121*, 6240–6257. <https://doi.org/10.1002/2015JD024680>
- Karoly, D. J. (1989). Southern Hemisphere circulation features associated with El Niño-Southern Oscillation events. *Journal of Climate*, *2*(11), 1239–1252.
- Kashiwase, H., Ohshima, K. I., Nihashi, S., & Eicken, H. (2017). Evidence for ice-ocean albedo feedback in the Arctic Ocean shifting to a seasonal ice zone. *Scientific Reports*, *7*(1), 8170. <https://doi.org/10.1038/s41598-017-08467-z>
- Kohyama, T., & Hartmann, D. L. (2016). Antarctic sea ice response to weather and climate modes of variability. *Journal of Climate*, *29*(2), 721–741.
- Kostov, Y., Marshall, J., Hausmann, U., Armour, K. C., Ferreira, D., & Holland, M. M. (2017). Fast and slow responses of Southern Ocean sea surface temperature to SAM in coupled climate models. *Climate Dynamics*, *48*(5), 1595–1609. Retrieved from <https://doi.org/10.1007/s00382-016-3162-z>
- Kusahara, K., Williams, G. D., Massom, R., Reid, P., & Hasumi, H. (2018). Spatiotemporal dependence of Antarctic sea ice variability to dynamic and thermodynamic forcing: A coupled ocean-sea ice model study. *Climate Dynamics*, *52*(7-8), 3791–3807. Retrieved from <https://doi.org/10.1007/s00382-018-4348-3>
- Kwok, R., Comiso, J. C., Lee, T., & Holland, P. (2016). Linked trends in the South Pacific sea ice edge and Southern Oscillation Index. *Geophysical Research Letters*, *43*, 10,295–10,302. <https://doi.org/10.1002/2016GL070655>. Received.
- Kwok, R., Pang, S. S., & Kacimi, S. (2017). Sea ice drift in the Southern Ocean: Regional patterns, variability, and trends. *Elementa: Science of the Anthropocene*, *5*, 32. Retrieved from <https://doi.org/10.1525/elementa.226>
- Large, W. G., & van Loon, H. (1989). Large scale, low frequency variability of the 1979 FGGE surface buoy drifts and winds over the Southern Hemisphere. *Journal of Physical Oceanography*, *19*, 216–232.
- Lefebvre, W., Goosse, H., Timmermann, R., & Fichefet, T. (2004). Influence of the Southern Annular Mode on the sea ice–ocean system. *Journal of Geophysical Research*, *109*, C09005. <https://doi.org/10.1029/2004JC002403>
- Li, X., Holland, D. M., Gerber, E. P., & Yoo, C. (2014). Impacts of the north and tropical Atlantic Ocean on the Antarctic Peninsula and sea ice. *Nature*, *505*(7484), 538–542.
- Liu, J., & Curry, J. A. (2010). Accelerated warming of the Southern Ocean and its impacts on the hydrological cycle and sea ice. *Proceedings of the National Academy of Sciences*, *107*(34), 14,987–14,992. Retrieved from <https://doi.org/10.1073/pnas.1003336107>
- Macalady, A., & Thomas, K. (Eds.) (2017). *Antarctic sea ice variability in the Southern Ocean-climate system: Proceedings of a workshop* Edited by Macalady, A., & Thomas, K. Washington, DC: The National Academies Press.
- Mahlstein, I., Gent, P. R., & Solomon, S. (2013). Historical Antarctic mean sea ice area, sea ice trends, and winds in CMIP5 simulations. *Journal of Geophysical Research: Atmospheres*, *118*, 5105–5110. <https://doi.org/10.1002/jgrd.50443>
- Maksym, T. (2019). Arctic and Antarctic sea ice change: Contrasts, commonalities, and causes. *Annual Review of Marine Science*, *11*, 187–213. Retrieved from (PMID: 30216739) <https://doi.org/10.1146/annurev-marine-010816-060610>
- Maksym, T., Stammerjohn, S., Ackley, S., & Massom, R. (2012). Antarctic sea ice—A polar opposite? *Oceanography*, *25*(3), 140–151. Retrieved from <https://doi.org/10.5670/oceanog.2012.88>
- Markus, T., & Cavalieri, D. J. (2000). An enhancement of the NASA Team sea ice algorithm. *IEEE Transactions on Geoscience and Remote Sensing*, *38*(3), 1387–1398.
- Marshall, G. J. (2003). Trends in the Southern Annular Mode from observations and reanalyses. *Journal of Climate*, *16*(24), 4134–4143. [https://doi.org/10.1175/1520-0442\(2003\)016<4134:TITSAM>2.0.CO;2](https://doi.org/10.1175/1520-0442(2003)016<4134:TITSAM>2.0.CO;2)
- Martinson, D. G. (1990). Evolution of the Southern Ocean winter mixed layer and sea ice: Open ocean deepwater formation and ventilation. *Journal of Geophysical Research*, *95*(C7), 11,641–11,654. <https://doi.org/10.1029/JC0095iC07p11641>
- Martinson, D. G. (2012). Antarctic circumpolar current's role in the Antarctic ice system: An overview. *Palaeogeography, Palaeoclimatology, Palaeoecology*, *335-336*, 71–74. Retrieved from <https://doi.org/10.1016/j.palaeo.2011.04.007>
- Massom, R., Reid, P., Stammerjohn, S., Raymond, B., Fraser, A., & Ushio, S. (2013). Change and variability in East Antarctic sea ice seasonality, 1979/80-2009/10. *PLoS ONE*, *8*(5), e64756. <https://doi.org/10.1371/journal.pone.0064756>
- Massom, R. A., Stammerjohn, S. E., Lefebvre, W., Harangozo, S. A., Adams, N., Scambos, T. A., et al. (2008). West Antarctic Peninsula sea ice in 2005: Extreme ice compaction and ice edge retreat due to strong anomaly with respect to climate. *Journal of Geophysical Research*, *113*, C02S20. <https://doi.org/10.1029/2007JC004239>
- Massonnet, F., Guemas, V., Fučkar, N. S., & Doblas-Reyes, F. J. (2015). The 2014 high record of Antarctic sea ice extent. *Bulletin of the American Meteorological Society*, *96*(12), S163–S167.
- Matear, R. J., O'Kane, T. J., Risbey, J. S., & Chamberlain, M. (2015). Sources of heterogeneous variability and trends in Antarctic sea-ice. *Nature Communications*, *6*, 8656. <https://doi.org/10.1038/ncomms9656>
- Mayewski, P. A., Meredith, M. P., Summerhayes, C. P., Turner, J., Worby, A., Barrett, P. J., et al. (2009). State of the Antarctic and Southern Ocean climate system. *Reviews of Geophysics*, *47*, RG1003. <https://doi.org/10.1029/2007RG000231>
- Maykut, G. A. (1986). The surface heat and mass balance. In N. Untersteiner (Ed.), *The geophysics of sea ice* (pp. 395–463). Boston, MA: Springer US. https://doi.org/10.1007/978-1-4899-5352-0_6
- Maykut, G. A., & McPhee, M. G. (1995). Solar heating of the Arctic mixed layer. *Journal of Geophysical Research*, *100*(C12), 24,691–24,703.
- Maykut, G. A., & Perovich, D. K. (1987). The role of shortwave radiation in the summer decay of a sea ice cover. *Journal of Geophysical Research*, *92*(C7), 7032–7044.

- Meehl, G. A. (1991). A reexamination of the mechanism of the semiannual oscillation in the Southern Hemisphere. *Journal of Climate*, 4(9), 911–926.
- Meehl, G. A., Arblaster, J. M., Bitz, C. M., Chung, C. T. Y., & Teng, H. (2016). Antarctic sea-ice expansion between 2000 and 2014 driven by tropical Pacific decadal climate variability. *Nature Geoscience*, 9(8), 590–595. <https://doi.org/10.1038/ngeo2751>
- Meehl, G. A., Arblaster, J. M., Chung, C. T., Holland, M. M., DuVivier, A., Thompson, L., et al. (2019). Sustained ocean changes contributed to sudden Antarctic sea ice retreat in late 2016. *Nature Communications*, 10(1), 14.
- Meehl, G. A., Hurrell, J. W., & van Loon, H. (1998). A modulation of the mechanism of the semiannual oscillation in the Southern Hemisphere. *Tellus, Series A: Dynamic Meteorology and Oceanography*, 50(4), 442–450. <https://doi.org/10.3402/tellusa.v50i4.14537>
- Meehl, G. A., Teng, H., & Arblaster, J. M. (2014). Climate model simulations of the observed early-2000s hiatus of global warming. *Nature Climate Change*, 4(10), 898–902.
- Meier, W. N., Gallaher, D., & Campbell, G. G. (2013). New estimates of Arctic and Antarctic sea ice extent during September 1964 from recovered Nimbus I satellite imagery. *The Cryosphere Discussions*, 7(1), 35–53. Retrieved from <https://doi.org/10.5194/tcd-7-35-2013>
- Meier, W. N., Khalsa, S. J. S., & Savoie, M. H. (2011). Intersensor calibration between F-13 SSM/I and F-17 SSMIS near-real-time sea ice estimates. *IEEE Transactions on Geoscience and Remote Sensing*, 49(9), 3343–3349.
- Meredith, M. P., & King, J. C. (2005). Rapid climate change in the ocean west of the Antarctic Peninsula during the second half of the 20th century. *Geophysical Research Letters*, 32, L19604. <https://doi.org/10.1029/2005GL024042>
- Mo, K. C. (2000). Relationships between low-frequency variability in the Southern Hemisphere and sea surface temperature anomalies. *Journal of Climate*, 13(20), 3599–3610.
- Mo, K. C., & Higgins, R. W. (1998). The Pacific–South American modes and tropical convection during the Southern Hemisphere winter. *Monthly Weather Review*, 126(6), 1581–1596.
- Mo, K. C., & Paegle, J. N. (2001). The Pacific–South American modes and their downstream effects. *International Journal of Climatology: A Journal of the Royal Meteorological Society*, 21(10), 1211–1229.
- Nan, S., & Li, J. (2003). The relationship between the summer precipitation in the Yangtze River Valley and the boreal spring Southern Hemisphere annular mode. *Geophysical Research Letters*, 30(24), 2266. <https://doi.org/10.1029/2003GL018381>
- Nihashi, S., & Cavalieri, D. J. (2006). Observational evidence of a hemispheric-wide ice–ocean albedo feedback effect on Antarctic sea-ice decay. *Journal of Geophysical Research*, 111, C12001. <https://doi.org/10.1029/2005JC003447>
- Nihashi, S., & Ohshima, K. I. (2001). Relationship between ice decay and solar heating through open water in the Antarctic sea ice zone. *Journal of Geophysical Research*, 106(C8), 16,767–16,782. <https://doi.org/10.1029/2000JC000399>
- Notz, D. (2014). Sea-ice extent and its trend provide limited metrics of model performance. *Cryosphere*, 8(1), 229–243. <https://doi.org/10.5194/tc-8-229-2014>
- Notz, D., & Stroeve, J. (2016). Observed Arctic sea-ice loss directly follows anthropogenic CO₂ emission. *Science (New York, N.Y.)*, 354(6313), 747–750. Retrieved from <https://doi.org/10.1126/science.aag2345>
- Ogura, T. (2004). Effects of sea ice dynamics on the Antarctic sea ice distribution in a coupled ocean atmosphere model. *Journal of Geophysical Research*, 109, C04025. <https://doi.org/10.1029/2003JC002022>
- Ohshima, K. I., & Nihashi, S. (2005). A simplified ice ocean coupled model for the Antarctic ice melt season. *Journal of Physical Oceanography*, 35, 188. <https://doi.org/10.1175/JPO-2675.1>
- Okumura, Y. M., Schneider, D., Deser, C., & Wilson, R. (2012). Decadal–interdecadal climate variability over Antarctica and linkages to the tropics: Analysis of ice core, instrumental, and tropical proxy data. *Journal of Climate*, 25(21), 7421–7441.
- Ozsoy-Cicek, B., Xie, H., Ackley, S. F., & Ye, K. (2009). Antarctic summer sea ice concentration and extent: Comparison of ODEN 2006 ship observations, satellite passive microwave and NIC sea ice charts. *The Cryosphere*, 3(1), 1–9. Retrieved from <https://doi.org/10.5194/tc-3-1-2009>
- Park, W., & Latif, M. (2018). Ensemble global warming simulations with idealized Antarctic meltwater input. *Climate Dynamics*, 52, 3223–3239.
- Parkinson, C. L. (2014). Global sea ice coverage from satellite data: Annual cycle and 35-yr trends. *Journal of Climate*, 27(24), 9377–9382. <https://doi.org/10.1175/JCLI-D-14-00605.1>
- Parkinson, C. L., & Cavalieri, D. J. (2012). Antarctic sea ice variability and trends, 1979–2010. *Cryosphere*, 6(4), 871–880. <https://doi.org/10.5194/tc-6-871-2012>
- Parkinson, C. L., & Washington, W. M. (1979). A large-scale numerical model of sea ice. *Journal of Geophysical Research*, 84, 311–337.
- Pauling, A. G., Smith, I. J., Langhorne, P. J., & Bitz, C. M. (2017). Time-dependent freshwater input from ice shelves: Impacts on Antarctic sea ice and the Southern Ocean in an Earth System Model. *Geophysical Research Letters*, 44, 10,454–10,461. <https://doi.org/10.1002/2017GL075017>
- Pezza, A. B., Rashid, H. A., & Simmonds, I. (2012). Climate links and recent extremes in Antarctic sea ice, high-latitude cyclones, Southern Annular Mode and ENSO. *Climate Dynamics*, 38(1–2), 57–73.
- Polvani, L. M., & Smith, K. L. (2013). Can natural variability explain observed Antarctic sea ice trends? *Geophysical Research Letters*, 40, 3195–3199. <https://doi.org/10.1002/grl.50578>
- Pope, J. O., Holland, P., Orr, A., Marshall, G. J., & Phillips, T. (2017). The impacts of El Niño on the observed sea ice budget of West Antarctica. *Geophysical Research Letters*, 44, 6200–6208. <https://doi.org/10.1002/2017GL073414>
- Raphael, M. N., & Hobbs, W. (2014). The influence of the large-scale atmospheric circulation on Antarctic sea ice during ice advance and retreat seasons. *Geophysical Research Letters*, 41, 5037–5045. <https://doi.org/10.1002/2014GL060365>
- Raphael, M. N., & Holland, M. M. (2006). Twentieth century simulation of the Southern Hemisphere climate in coupled models. Part 1: Large scale circulation variability. *Climate Dynamics*, 26(2–3), 217–228. <https://doi.org/10.1007/s00382-005-0082-8>
- Raphael, M. N., Marshall, G. J., Turner, J., Fogt, R. L., Schneider, D., Dixon, D. A., et al. (2016). The Amundsen Sea low: Variability, change, and impact on Antarctic climate. *Bulletin of the American Meteorological Society*, 97(1), 111–121. <https://doi.org/10.1175/BAMS-D-14-00018.1>
- Renwick, J. A., Kohout, A., & Dean, S. (2012). Atmospheric forcing of Antarctic sea ice on intraseasonal time scales. *Journal of Climate*, 25(17), 5962–5975.
- Reuter, F. (1936). *Die synoptische Darstellung der 1/2-jährigen Druckwelle*. Leipzig: Geophysik. Inst. d. Univ.
- Roach, L. A., Dean, S. M., & Renwick, J. A. (2018). Consistent biases in Antarctic sea ice concentration simulated by climate models. *The Cryosphere*, 12(1), 365–383. Retrieved from <https://doi.org/10.5194/tc-12-365-2018>
- Rosenblum, E., & Eisenman, I. (2017). Sea ice trends in climate models only accurate in runs with biased global warming. *Journal of Climate*, 30(16), 6265–6278.
- Russell, J. L., Stouffer, R. J., & Dixon, K. W. (2006). Intercomparison of the Southern Ocean circulations in IPCC coupled model control simulations. *Journal of Climate*, 19(18), 4560–4575. Retrieved from <https://doi.org/10.1175/JCLI3869.1>

- Schemm, S. (2018). Regional trends in weather systems help explain Antarctic sea ice trends. *Geophysical Research Letters*, *45*, 7165–7175. <https://doi.org/10.1029/2018GL079109>
- Schlosser, E., Haumann, F. A., & Raphael, M. N. (2018). Atmospheric influences on the anomalous 2016 Antarctic sea ice decay. *Cryosphere*, *12*(3), 1103–1119.
- Schneider, D. P., & Steig, E. J. (2008). Ice cores record significant 1940s Antarctic warmth related to tropical climate variability. *Proceedings of the National Academy of Sciences*, *105*(34), 12,154–12,158.
- Schwerdtfeger, W. (1960). The seasonal variation of the strength of the southern circumpolar vortex. *Monthly Weather Review*, *88*(6), 203.
- Schwerdtfeger, W. (1963). *The southern circumpolar vortex and the spring warming of the polar stratosphere*, Meteorologische Abhandlungen (Vol. 36, pp. 207–224). Dietrich Reimer.
- Shu, Q., Song, Z., & Qiao, F. (2015). Assessment of sea ice simulations in the CMIP5 models. *Cryosphere*, *9*(1), 399–409. <https://doi.org/10.5194/tc-9-399-2015>
- Sigmond, M., & Fyfe, J. C. (2010). Has the ozone hole contributed to increased Antarctic sea ice extent? *Geophysical Research Letters*, *37*, L18502. <https://doi.org/10.1029/2010GL044301>
- Simmonds, I., & Jacka, T. H. (1995). Relationships between the interannual variability of Antarctic sea ice and the Southern Oscillation. *Journal of Climate*, *8*(3), 637–647.
- Simmonds, I., & Jones, D. A. (1998). The mean structure and temporal variability of the semiannual oscillation in the southern extratropics. *International Journal of Climatology*, *18*(5), 473–504. [https://doi.org/10.1002/\(SICI\)1097-0088\(199804\)18:5<473::AID-JOC266>3.0.CO;2-0](https://doi.org/10.1002/(SICI)1097-0088(199804)18:5<473::AID-JOC266>3.0.CO;2-0)
- Simmonds, I., & Kevin (2000). Mean Southern Hemisphere extratropical cyclone behavior in the 40-Year NCEPNCAR Reanalysis. *Journal of Climate*, *13*(5), 873–885. [https://doi.org/10.1175/1520-0442\(2000\)013<0873:MSHECB>2.0.CO;2](https://doi.org/10.1175/1520-0442(2000)013<0873:MSHECB>2.0.CO;2)
- Simmonds, I., Keay, K., & Lim, E.-P. (2003). Synoptic activity in the seas around Antarctica. *Monthly Weather Review*, *131*(2), 272–288.
- Simpkins, G. R., Ciasto, L. M., & England, M. H. (2013). Observed variations in multidecadal Antarctic sea ice trends during 1979–2012. *Geophysical Research Letters*, *40*, 3643–3648. <https://doi.org/10.1002/grl.50715>
- Simpkins, G. R., McGregor, S., Taschetto, A. S., Ciasto, L. M., & England, M. H. (2014). Tropical connections to climatic change in the extratropical Southern Hemisphere: The role of Atlantic SST trends. *Journal of Climate*, *27*(13), 4923–4936.
- Stammerjohn, S. E., Drinkwater, M. R., Smith, R. C., & Liu, X. (2003). Ice-atmosphere interactions during sea-ice advance and retreat in the western Antarctic Peninsula region. *Journal of Geophysical Research*, *108*(C10), 3329. <https://doi.org/10.1029/2002JC001543>
- Stammerjohn, S. E., Martinson, D. G., Smith, R. C., Yuan, X., & Rind, D. (2008). Trends in Antarctic annual sea ice retreat and advance and their relation to El Niño–Southern Oscillation and Southern Annular Mode variability. *Journal of Geophysical Research*, *113*, C03S90. Retrieved from <https://doi.org/10.1029/2007JC004269>
- Stammerjohn, S., Massom, R., Rind, D., & Martinson, D. G. (2012). Regions of rapid sea ice change: An inter-hemispheric seasonal comparison. *Geophysical Research Letters*, *39*, L06501. <https://doi.org/10.1029/2012GL050874>
- Sterl, A., van Oldenborgh, G. J., Hazeleger, W., & Burgers, G. (2007). On the robustness of ENSO teleconnections. *Climate Dynamics*, *29*(5), 469–485.
- Stroeve, J., Jenouvrier, S., Campbell, G. G., Barbraud, C., & Delord, K. (2016). Mapping and assessing variability in the Antarctic marginal ice zone, pack ice and coastal polynyas in two sea ice algorithms with implications on breeding success of snow petrels. *Cryosphere*, *10*(4), 1823–1843. <https://doi.org/10.5194/tc-10-1823-2016>
- Stroeve, J. C., Markus, T., Boisvert, L., Miller, J., & Barrett, A. (2014). Changes in Arctic melt season and implications for sea ice loss. *Geophysical Research Letters*, *41*, 1216–1225. <https://doi.org/10.1002/2013GL058951>
- Stroeve, J., & Notz, D. (2018). Changing state of Arctic sea ice across all seasons Changing state of Arctic sea ice across all seasons. *Environmental Research Letters*, *13*, 103001. <https://doi.org/10.1088/1748-9326/aade56>
- Taschetto, A., Wainer, I., & Raphael, M. (2007). Interannual variability associated with Semiannual Oscillation in southern high latitudes. *Journal of Geophysical Research*, *112*, D02106. <https://doi.org/10.1029/2006JD007648>
- Thompson, D. W. J., & Solomon, S. (2002). Interpretation of recent Southern Hemisphere climate change. *Science*, *296*, 895–899. <https://doi.org/10.1126/science.1069270>
- Thompson, D. W. J., & Wallace, J. M. (2000). Annular modes in the extratropical circulation. Part I: Month-to-month variability. *Journal of climate*, *13*(5), 1000–1016.
- Trenberth, K. E. (1991). Storm tracks in the Southern Hemisphere. *Journal of the Atmospheric Sciences*, *48*(19), 2159–2178. [https://doi.org/10.1175/1520-0469\(1991\)048<2159:STTISH>2.0.CO;2](https://doi.org/10.1175/1520-0469(1991)048<2159:STTISH>2.0.CO;2)
- Trenberth, K. E., Large, W. G., & Olson, J. G. (1990). The mean annual cycle in global ocean wind stress. *Journal of Physical Oceanography*, *20*, 1742–1760.
- Turner, J. (2004). The El Niño–Southern Oscillation and Antarctica. *International Journal of Climatology: A Journal of the Royal Meteorological Society*, *24*(1), 1–31.
- Turner, J., Bracegirdle, T. J., Phillips, T., Marshall, G. J., & Scott Hosking, J. (2012). An initial assessment of Antarctic sea ice extent in the CMIP5 models. *Journal of Climate*, *26*(5), 1473–1484. <https://doi.org/10.1175/JCLI-D-12-00068.1>
- Turner, J., Hosking, J. S., Bracegirdle, T. J., Marshall, G. J., & Phillips, T. (2015). Recent changes in Antarctic sea ice. *Philosophical Transactions of the Royal Society A*, *373*(2045), 20140163.
- Turner, J., Hosking, J. S., Phillips, T., & Marshall, G. J. (2013). Temporal and spatial evolution of the Antarctic sea ice prior to the September 2012 record maximum extent. *Geophysical Research Letters*, *40*, 5894–5898. <https://doi.org/10.1002/2013GL058371>
- Turner, J., Marshall, G. J., & Lachlan-Cope, T. A. (1998). Analysis of synoptic-scale low pressure systems within the Antarctic Peninsula sector of the circumpolar trough. *International Journal of Climatology*, *18*(3), 253–280.
- Turner, J., Phillips, T., Hosking, J. S., Marshall, G. J., & Orr, A. (2013). The Amundsen Sea low. *International Journal of Climatology*, *33*(7), 1818–1829.
- Turner, J., Phillips, T., Marshall, G. J., Hosking, J. S., Pope, J. O., Bracegirdle, T. J., & Deb, P. (2017). Unprecedented springtime retreat of Antarctic sea ice in 2016. *Geophysical Research Letters*, *44*, 6868–6875. Retrieved from <https://doi.org/10.1002/2017GL073656>
- Turner, J., Scott Hosking, J., Marshall, G. J., Phillips, T., & Bracegirdle, T. J. (2016). Antarctic sea ice increase consistent with intrinsic variability of the Amundsen sea low. *Climate Dynamics*, *46*(7–8), 2391–2402. <https://doi.org/10.1007/s00382-015-2708-9>
- van Loon, H. (1967). The half-yearly oscillations in middle and high southern latitudes and the coreless winter. *Journal of the Atmospheric Sciences*, *24*, 472–486. [https://doi.org/10.1175/1520-0469\(1967\)024<0472:THYOIM>2.0.CO;2](https://doi.org/10.1175/1520-0469(1967)024<0472:THYOIM>2.0.CO;2)
- van Loon, H., & Jenne, R. L. (1972). The zonal harmonic standing waves in the Southern Hemisphere. *Journal of Geophysical Research*, *77*(6), 992–1003. <https://doi.org/10.1029/JC077i006p00992>

- van Loon, H., & Rogers, J. C. (1984). Interannual variations in the half-yearly cycle of pressure gradients and zonal wind at sea level on the Southern Hemisphere. *Tellus, Series A: Dynamic Meteorology and Oceanography*, 36(1), 76–86. <https://doi.org/10.3402/tellusa.v36i1.11467>
- van den Broeke, M. R. (1998). The semi-annual oscillation and Antarctic climate. Part 2: Recent changes. *Antarctic Science*, 10(2), 184–191. <https://doi.org/10.1017/S095410209800025X>
- Visbeck, M. (2009). A station-based Southern Annular Mode index from 1884 to 2005. *Journal of Climate*, 22(4), 940–950.
- Walland, D., & Simmonds, I. (1999). Baroclinicity, meridional temperature gradients, and the southern semiannual oscillation. *Journal of Climate*, 12, 3376–3382.
- Walsh, J. E., & Johnson, C. M. (1979). An analysis of Arctic sea ice fluctuations, 1953–77. *Journal of Physical Oceanography*, 9(3), 580–591.
- Wang, G., Hendon, H. H., Arblaster, J. M., Lim, E.-P., Abhik, S., & van Rensch, P. (2019). Compounding tropical and stratospheric forcing of the record low Antarctic sea-ice in 2016. *Nature communications*, 10(1), 13.
- Watkins, A. B., & Simmonds, I. (1999). A late spring surge in the open water of the Antarctic sea ice pack. *Geophysical Research Letters*, 26(10), 1481–1484. <https://doi.org/10.1029/1999GL900292>
- Wilson, E. A., Riser, S. C., Campbell, E. C., & Wong, A. P. (2019). Winter upper ocean stability and ice-ocean feedbacks in the sea-ice-covered Southern Ocean. *Journal of Physical Oceanography*, 49, 1099–1117.
- Worby, A. P., Geiger, C. A., Paget, M. J., van Woert, M. L., Ackley, S. F., & DeLiberty, T. L. (2008). Thickness distribution of Antarctic sea ice. *Journal of Geophysical Research*, 113, C05S92. <https://doi.org/10.1029/2007JC004254>
- Xu, J.-S., von Storch, H., & van Loon, H. (1990). The performance of four spectral GCMs in the Southern Hemisphere: The January and July climatology and the seminannual wave. *Journal of Climate*, 3, 53–70.
- Yu, L., Zhang, Z., Zhou, M., Zhong, S., Lenschow, D. H., Gao, Z., et al. (2011). Interpretation of recent trends in Antarctic sea ice concentration. *Journal of Applied Remote Sensing*, 5, 053557. <https://doi.org/10.1117/1.3643691>
- Yuan, X. (2004). ENSO-related impacts on Antarctic sea ice: A synthesis of phenomenon and mechanisms. *Antarctic Science*, 16(4), 415–425.
- Yuan, X., & Li, C. (2008). Climate modes in southern high latitudes and their impacts on Antarctic sea ice. *Journal of Geophysical Research*, 113, C06S91. <https://doi.org/10.1029/2006JC004067>
- Zhang, J. (2007). Increasing Antarctic sea ice under warming atmospheric and oceanic conditions. *Journal of Climate*, 20(11), 2515–2529.
- Zunz, V., Goosse, H., & Massonnet, F. (2013). How does internal variability influence the ability of CMIP5 models to reproduce the recent trend in Southern Ocean sea ice extent? *Cryosphere*, 7(2), 451–468. <https://doi.org/10.5194/tc-7-451-2013>
- Zwally, H. J., Comiso, J. C., Parkinson, C. L., Campbell, W. J., & Carsey, F. D. (1983). Antarctic sea ice, 1973-1976: Satellite passive-microwave observations (Tech. Rep.). Washington DC: National Aeronautics and Space Administration.